Bounding Integrity Risk for Sequential State Estimators in the Presence of Stochastic Modeling Uncertainty

Steven E. Langel [1] and Samer M. Khanafseh [2]
Illinois Institute of Technology, Chicago, Illinois, 60616

Boris S. Pervan [3]
Illinois Institute of Technology, Chicago, Illinois, 60616

A new method is introduced to upper bound integrity risk for sequential state estimators when the autocorrelation functions of measurement noise and disturbance inputs are subject to bounded uncertainties. Integrity risk is defined as the probability of the state estimate error exceeding predefined bounds of acceptability. In the first part of the paper, a new expression is derived that relates the measurement noise and disturbance input autocorrelation functions to the state estimate error vector. Using this relation, an efficient algorithm is developed in the second part of the paper to upper bound the estimation integrity risk when each input autocorrelation function is known to lie between upper and lower bounding functions. Numerical simulations for a one-dimensional position and velocity estimation problem are conducted to demonstrate the practical feasibility and effectiveness of this new bounding method.

I. Introduction

FOR estimation applications where the state vector evolves according to a dynamic model, measurements are typically processed (or filtered) over time. The Kalman filter is the most widely used algorithm for recursive state vector estimation. One of the fundamental assumptions used in the derivation of the Kalman filter is that the measurement and disturbance inputs are white noise sequences. In general, these random processes will be time correlated, which must be properly accounted for in the estimation algorithm. State augmentation is one well-known approach that can be used to account for time correlation by using additional filter states [1]. The resulting increase

[1] PhD Candidate, Department of Mechanical, Materials and Aerospace Engineering, E-mail: langste@hawk.iit.edu.
[2] Research Assistant Professor, Department of Mechanical, Materials and Aerospace Engineering, E-mail: khansam1@iit.edu, AIAA Member.
[3] Professor, Department of Mechanical, Materials and Aerospace Engineering, E-mail: pervan@iit.edu, Associate Fellow AIAA.

in state vector dimension can sometimes have adverse practical ramifications, and this has resulted in alternative solutions that do not require additional states. Two examples of such alternatives are the measurement differencing filter [2] and the Schmidt-Kalman filter [3]. Because the choice of which method to use is mainly a practical consideration, this work will use the standard state augmentation paradigm to account for time correlation. Irrespective of which method is used, perfect knowledge of the measurement noise and disturbance input autocorrelation functions must be available. Since the true mathematical nature of these functions is rarely known, approximate, reduced order models are often employed. For safety-critical estimation applications, such as aircraft navigation, it is essential to understand how the use of approximate models affects integrity risk.

In the aircraft navigation community, an abundance of research has addressed the issue of uncertainty in characterizing measurement noise. For example, in [4] and [5], it is shown how to compute an upper bound on integrity risk using the concept of cumulative distribution function (CDF) overbounding. These results apply for the special case where measurement errors are mutually independent. However, when state estimation is accomplished through measurement filtering, the presence of any time correlation in the measurement noise violates the independence assumption. In response, in [6] and [7] the symmetric overbounding theorem was developed to generalize CDF overbounding techniques to the case where measurement errors are correlated. The theorem provides a solid theoretical foundation for integrity risk bounding with correlated errors but does not provide a readily implementable solution. This paper uses key ideas from [6] and [7] to derive an efficient integrity risk bounding algorithm for the Kalman filter.

In parallel, numerous publications in the robust estimation literature can be found that address the integrity risk bounding problem for specialized cases of modeling uncertainty. For example, in [8] and [9], it is shown how to upper bound integrity risk when the measurement noise is governed by a first order Gauss-Markov model with an unknown time constant. More general uncertainty structures can be handled using guaranteed cost filtering [10], where a linear estimator is sought such that the estimate error variance is guaranteed to be smaller than a certain bound. The design matrices are chosen to minimize the upper bound subject to a specified uncertainty structure on the state transition matrix and observation matrix.

Norm-bounded uncertainty is one type of uncertainty structure that has been studied extensively using guaranteed cost filtering [11-14]. Under this structural model, the minimum upper bound on the estimate error variance is obtained by solving algebraic Riccati equations (AREs). The polytopic uncertainty structure is another

example, where the state transition matrix and observation matrix are expressed as unknown linear combinations of a set of matrices [15-20]. The advantage of this formulation is that the robust filtering problem can be written in terms of Linear Matrix Inequalities (LMIs), which can be solved efficiently using existing algorithms [21]. For a thorough overview of norm bounded and polytopic uncertainty, the reader is referred to [10] and [22].

Guaranteed cost filtering is an effective solution to the integrity risk bounding problem provided that the size of the state transition matrix is known a priori. However, when the statistical models of the measurement noise and disturbance inputs are not precisely known, the number of states necessary to accurately model these processes is also unknown. Futhermore, certain noise processes like flicker noise in quartz oscillators cannot even be modeled with a finite number of states [23]. These problems cannot be addressed using guaranteed cost filtering. In response, this paper introduces a new approach to upper bound integrity risk that only requires each measurement noise and disturbance input autocorrelation function to be contained between an upper and lower bounding function.

In section II, the basics of Kalman filtering are reviewed with emphasis on the method of state augmentation for time correlated noise processes. The concept of estimation integrity risk is then formally introduced and the role of the estimate error variance in its computation is discussed. In section III, a set of difference equations is derived that explicitly shows how the time correlated measurement noise and disturbance inputs impact the state estimate error vector. Section IV derives an efficient algorithm to upper bound the integrity risk subject to the bounded autocorrelation uncertainty structure. In section V the algorithms and methods developed in the paper are applied to a one-dimensional position and velocity estimation application.

II. Time Correlated Noise in Kalman Filters

A. Measurement and State Dynamic Models

This work is concerned with linear measurement models of the form

$$\mathbf{z}_k = \mathbf{H}_{\theta,k}\,\boldsymbol{\theta}_k + \mathbf{J}_{\nu,k}\,\boldsymbol{\nu}_k \tag{1}$$

where $\mathbf{z}_k$ is the $n_z \times 1$ measurement vector, $\mathbf{H}_{\theta,k}$ is the $n_z \times n_\theta$ observation matrix, $\boldsymbol{\theta}_k$ is the $n_\theta \times 1$ state vector, $\mathbf{J}_{\nu,k}$ is the $n_z \times n_\nu$ measurement noise mapping matrix and $\boldsymbol{\nu}_k$ is an $n_\nu \times 1$ zero-mean Gaussian random noise vector. The subscript k indicates that a quantity is defined at time index k.

The state vector $\boldsymbol{\theta}$ evolves in time according to the linear dynamic model

$$\boldsymbol{\theta}_{k+1} = \mathbf{F}_{\theta,k}\,\boldsymbol{\theta}_k + \mathbf{G}_{\theta,k}\,\boldsymbol{w}_k \tag{2}$$

where $\mathbf{F}_{\theta,k}$ is the $n_\theta \times n_\theta$ state transition matrix, $\mathbf{G}_{\theta,k}$ is the $n_\theta \times n_w$ disturbance input mapping matrix and $\boldsymbol{w}_k$ is an $n_w \times 1$ zero-mean Gaussian random noise vector.

In this work, $\mathbf{H}_{\theta,k}$, $\mathbf{J}_{\nu,k}$, $\mathbf{F}_{\theta,k}$ and $\mathbf{G}_{\theta,k}$ are assumed to be precisely known matrices and the noise vectors $\boldsymbol{\nu}$ and $\boldsymbol{w}$ are statistically modeled as

$$E[\boldsymbol{\nu}_k \boldsymbol{\nu}_l^T]_{ij} = \overset{\nu}{r}_{i,k-l}\,\delta_{ij} \quad , \quad \begin{matrix} i = 1, \cdots, n_\nu \\ j = 1, \cdots, n_\nu \end{matrix} \tag{3}$$

$$E[\boldsymbol{w}_k \boldsymbol{w}_l^T]_{ij} = \overset{w}{r}_{i,k-l}\,\delta_{ij} \quad , \quad \begin{matrix} i = 1, \cdots, n_w \\ j = 1, \cdots, n_w \end{matrix} \tag{4}$$

$$E[\boldsymbol{w}_k \boldsymbol{\nu}_l^T]_{ij} = \mathbf{0} \quad , \quad \begin{matrix} i = 1, \cdots, n_w \\ j = 1, \cdots, n_\nu \end{matrix} \tag{5}$$

where E is the expectation operator, k and l are time indices, i and j are matrix row and column indices, respectively, and δ_{ij} is the Kronecker delta.

Let $\{\boldsymbol{\nu}_i\}$ denote a time series of arbitrary length of the i^{th} component of $\boldsymbol{\nu}$ and $\{\boldsymbol{w}_i\}$ denote a time series of arbitrary length of the i^{th} component of $\boldsymbol{w}$. Then $\overset{\nu}{r}_{i,k-l}$ is the value of the autocorrelation function of $\{\boldsymbol{\nu}_i\}$ at a time shift of $k - l$ and $\overset{w}{r}_{i,k-l}$ is the value of the autocorrelation function of $\{\boldsymbol{w}_i\}$ at a time shift of $k - l$. In general, $\overset{\nu}{r}_{i,k-l}$ and $\overset{w}{r}_{i,k-l}$ are non-zero for $k \neq l$, which indicates that there is time correlation in $\{\boldsymbol{\nu}_i\}$ and $\{\boldsymbol{w}_i\}$. However, the use of the Kronecker deltas in Eqs. (3) and (4) along with Eq. (5) stipulates that there is no cross correlation among the components of $\boldsymbol{\nu}$ and $\boldsymbol{w}$.

B. Method of State Augmentation

If $\boldsymbol{\nu}$ and $\boldsymbol{w}$ can be dynamically modeled as the output of a linear system driven by white Gaussian noise, then the well known method of state augmentation can be utilized to recast Eqs. (1) through (5) in the form of an estimation problem amenable to a Kalman filtering solution.

Suppose that $\boldsymbol{\nu}_k$ and $\boldsymbol{w}_k$ can be linearly decomposed as

$$\boldsymbol{\nu}_k = \mathbf{C}_k \boldsymbol{\eta}_k + \mathbf{D}_k \boldsymbol{r}_k \tag{6}$$

$$\boldsymbol{w}_k = \mathbf{A}_k \boldsymbol{\xi}_k + \mathbf{B}_k \boldsymbol{q}_{\theta,k} \tag{7}$$

where $\mathbf{C}_k$ is an $n_\nu \times n_\eta$ matrix, $\boldsymbol{\eta}$ is an $n_\eta \times 1$ zero-mean Gaussian random vector, $\mathbf{D}_k$ is an $n_\nu \times n_r$ matrix and $\boldsymbol{r}$ is an $n_r \times 1$ zero-mean white Gaussian random vector with $n_r \times n_r$ covariance matrix $E[\boldsymbol{r}_k \boldsymbol{r}_l^T] = \mathbf{R}_k \delta_{kl}$. Similarly, $\mathbf{A}_k$ is an $n_w \times n_\xi$ matrix, $\boldsymbol{\xi}$ is an $n_\xi \times 1$ zero-mean Gaussian random vector, $\mathbf{B}_k$ is an $n_w \times n_{q,\theta}$ matrix and $\boldsymbol{q}_\theta$ is an $n_{q,\theta} \times 1$ zero-mean white Gaussian random vector with $n_{q,\theta} \times n_{q,\theta}$ covariance matrix $E[\boldsymbol{q}_{\theta,k} \boldsymbol{q}_{\theta,l}^T] = \mathbf{Q}_{\theta,k} \delta_{kl}$.

It is assumed that $\boldsymbol{\eta}$ is uncorrelated with $\boldsymbol{r}$ and that $\boldsymbol{\xi}$ is uncorrelated with $\boldsymbol{q}_\theta$, i.e., $E[\boldsymbol{\eta}_k \boldsymbol{r}_l^T] = \mathbf{0}$ and $E[\boldsymbol{\xi}_k \boldsymbol{q}_{\theta,l}^T] = \mathbf{0}$ for all *k* and *l*. The vectors $\boldsymbol{\eta}$ and $\boldsymbol{\xi}$ capture the time correlated nature of $\boldsymbol{\nu}$ and $\boldsymbol{w}$, respectively, and evolve in time according to the linear dynamic models

$$\boldsymbol{\eta}_{k+1} = \mathbf{F}_{\eta,k} \boldsymbol{\eta}_k + \mathbf{G}_{\eta,k} \boldsymbol{q}_{\eta,k} \tag{8}$$

$$\boldsymbol{\xi}_{k+1} = \mathbf{F}_{\xi,k} \boldsymbol{\xi}_k + \mathbf{G}_{\xi,k} \boldsymbol{q}_{\xi,k} \tag{9}$$

where $\mathbf{F}_{\eta,k}$ is an $n_\eta \times n_\eta$ matrix, $\mathbf{G}_{\eta,k}$ is an $n_\eta \times n_{q,\eta}$ matrix, $\boldsymbol{q}_\eta$ is an $n_{q,\eta} \times 1$ zero-mean white Gaussian random vector with $n_{q,\eta} \times n_{q,\eta}$ covariance matrix $E[\boldsymbol{q}_{\eta,k} \boldsymbol{q}_{\eta,l}^T] = \mathbf{Q}_{\eta,k} \delta_{kl}$, $\mathbf{F}_{\xi,k}$ is an $n_\xi \times n_\xi$ matrix, $\mathbf{G}_{\xi,k}$ is an $n_\xi \times n_{q,\xi}$ matrix and $\boldsymbol{q}_\xi$ is an $n_{q,\xi} \times 1$ zero-mean white Gaussian random vector with $n_{q,\xi} \times n_{q,\xi}$ covariance matrix $E[\boldsymbol{q}_{\xi,k} \boldsymbol{q}_{\xi,l}^T] = \mathbf{Q}_{\xi,k} \delta_{kl}$.

Substituting Eq. (7) into Eq. (2) and appending Eqs. (8) and (9) to Eq. (2) results in the new linear dynamic model

$$\begin{bmatrix} \boldsymbol{\theta}_{k+1} \\ \boldsymbol{\xi}_{k+1} \\ \boldsymbol{\eta}_{k+1} \end{bmatrix} = \begin{bmatrix} \mathbf{F}_{\theta,k} & \mathbf{G}_{\theta,k}\mathbf{A}_k & \mathbf{0} \\ \mathbf{0} & \mathbf{F}_{\xi,k} & \mathbf{0} \\ \mathbf{0} & \mathbf{0} & \mathbf{F}_{\eta,k} \end{bmatrix} \begin{bmatrix} \boldsymbol{\theta}_k \\ \boldsymbol{\xi}_k \\ \boldsymbol{\eta}_k \end{bmatrix} + \begin{bmatrix} \mathbf{G}_{\theta,k}\mathbf{B}_k & \mathbf{0} & \mathbf{0} \\ \mathbf{0} & \mathbf{G}_{\xi,k} & \mathbf{0} \\ \mathbf{0} & \mathbf{0} & \mathbf{G}_{\eta,k} \end{bmatrix} \begin{bmatrix} \boldsymbol{q}_{\theta,k} \\ \boldsymbol{q}_{\xi,k} \\ \boldsymbol{q}_{\eta,k} \end{bmatrix} \tag{10}$$

which can be written more succinctly as $\boldsymbol{x}_{k+1} = \mathbf{F}_k \boldsymbol{x}_k + \mathbf{G}_k \boldsymbol{q}_k$. Defining $n_x = n_\theta + n_\eta + n_\xi$ and $n_q = n_{q,\theta} + n_{q,\eta} + n_{q,\xi}$, $\boldsymbol{x}_k$ is the $n_x \times 1$ state vector, $\mathbf{F}_k$ is the $n_x \times n_x$ state transition matrix, $\mathbf{G}_k$ is an $n_x \times n_q$ matrix and $\boldsymbol{q}$ is an $n_q \times 1$ zero-mean white Gaussian random vector with $n_q \times n_q$ covariance matrix

$$\mathbf{Q}_k = E[\boldsymbol{q}_k \boldsymbol{q}_l^T] = \begin{bmatrix} \mathbf{Q}_{\theta,k} & \mathbf{0} & \mathbf{0} \\ \mathbf{0} & \mathbf{Q}_{\xi,k} & \mathbf{0} \\ \mathbf{0} & \mathbf{0} & \mathbf{Q}_{\eta,k} \end{bmatrix} \delta_{kl}. \tag{11}$$

Inserting Eq. (6) into Eq. (1) and defining the $n_z \times n_x$ matrix $\mathbf{H}_k = [\, \mathbf{H}_{\theta,k} \quad \mathbf{0} \quad \mathbf{J}_{\nu,k}\mathbf{C}_k \,]$ and the $n_z \times n_r$ matrix $\mathbf{J}_k = \mathbf{J}_{\nu,k}\mathbf{D}_k$ results in the measurement model $\boldsymbol{z}_k = \mathbf{H}_k \boldsymbol{x}_k + \mathbf{J}_k \boldsymbol{r}_k$. An optimal estimate of the state vector $\boldsymbol{x}$ can now be obtained using the Kalman filter.

C. State Estimation Via Kalman Filtering

The Kalman filter is composed of a measurement update, producing the estimate vector $\hat{\boldsymbol{x}}_k = \hat{\boldsymbol{x}}_k^- + \mathbf{K}_k(\boldsymbol{z}_k - \mathbf{H}_k \hat{\boldsymbol{x}}_k^-)$, and a time update, which yields the estimate vector $\hat{\boldsymbol{x}}_{k+1}^- = \mathbf{F}_k \hat{\boldsymbol{x}}_k$ (Ref. 24). The vectors $\hat{\boldsymbol{x}}_k$, $\hat{\boldsymbol{x}}_k^-$ and $\hat{\boldsymbol{x}}_{k+1}^-$ have dimension $n_x \times 1$ and the Kalman gain matrix $\mathbf{K}_k$ (to be defined shortly) has dimension $n_x \times n_z$. The estimate error vectors associated with $\hat{\boldsymbol{x}}_k$ and $\hat{\boldsymbol{x}}_{k+1}^-$ are defined as $\boldsymbol{\varepsilon}_k = \hat{\boldsymbol{x}}_k - \boldsymbol{x}_k$ and $\boldsymbol{\varepsilon}_{k+1}^- = \hat{\boldsymbol{x}}_{k+1}^- - \boldsymbol{x}_{k+1}$, respectively, whose covariance matrices are determined from the expressions [24]

$$\hat{\mathbf{P}}_k = E[\boldsymbol{\varepsilon}_k \boldsymbol{\varepsilon}_k^T] = (\mathbf{I} - \mathbf{K}_k \mathbf{H}_k)\hat{\mathbf{P}}_k^- \tag{12}$$

$$\hat{\mathbf{P}}_{k+1}^- = E[\boldsymbol{\varepsilon}_{k+1}^- \boldsymbol{\varepsilon}_{k+1}^{-T}] = \mathbf{F}_k \hat{\mathbf{P}}_k \mathbf{F}_k^T + \mathbf{G}_k \mathbf{Q}_k \mathbf{G}_k^T \tag{13}$$

$$\mathbf{K}_k = \hat{\mathbf{P}}_k^- \mathbf{H}_k^T (\mathbf{H}_k \hat{\mathbf{P}}_k^- \mathbf{H}_k^T + \mathbf{J}_k \mathbf{R}_k \mathbf{J}_k^T)^{-1} \tag{14}$$

where $\hat{\mathbf{P}}_k^-$ ($n_x \times n_x$) is output during the time update and $\hat{\mathbf{P}}_k$ ($n_x \times n_x$) is output during the measurement update.

Throughout the paper, $\boldsymbol{\varepsilon}^-$ and $\boldsymbol{\varepsilon}$ will commonly be referred to as the a priori and a posteriori estimate error vectors, respectively. Both $\boldsymbol{\varepsilon}^-$ and $\boldsymbol{\varepsilon}$ are Gaussian random vectors as a result of the Gaussianity of $\boldsymbol{r}$ and $\boldsymbol{q}$ and the fact that the Kalman filter is an unbiased linear estimator. Therefore, Eqs. (12) and (13) completely specify the joint probability density function of the state estimate error vector after a measurement update and time update of the Kalman filter. $\hat{\mathbf{P}}_k$ and $\hat{\mathbf{P}}_{k+1}^-$ play a critical role in verifying that the likelihood of entering a hazardous situation is acceptably small for safety-critical estimation applications.

D. Definition of Integrity Risk

Let y be any scalar linear combination of $\boldsymbol{x}$ whose a posteriori estimate error is ε_y. That is, $y = \boldsymbol{\alpha}_y^T \boldsymbol{x}$ and $\varepsilon_y = \boldsymbol{\alpha}_y^T \boldsymbol{\varepsilon}$, where $\boldsymbol{\alpha}_y$ is a known $n_x \times 1$ vector. The estimation integrity risk of *y* is defined as

$$I_y = P(\varepsilon_y \notin [-\ell_y, \ell_y]) \tag{15}$$

where ℓ_y is a specified number.

Given that ε_y is a zero-mean Gaussian random variable, I_y evaluates to $I_y = \operatorname{erfc}\left(\ell_y \Big/ \sqrt{2\hat{\sigma}_y^2}\right)$, where $\hat{\sigma}_y^2$ is the variance of ε_y obtained from the covariance transformation $\hat{\sigma}_y^2 = \boldsymbol{\alpha}_y^T \hat{\mathbf{P}} \boldsymbol{\alpha}_y$. The a priori integrity risk is computed in an analogous manner by replacing $\hat{\sigma}_y^2$ with $\hat{\sigma}_y^{-2}$ and $\hat{\mathbf{P}}$ with $\hat{\mathbf{P}}^-$.

It is clear that the evaluation of I_y is straightforward once $\hat{\mathbf{P}}$ has been specified. However, it was shown in section B that when the components of $\boldsymbol{v}$ and $\boldsymbol{w}$ are time correlated, dynamic models for $\boldsymbol{v}$ and $\boldsymbol{w}$ needed to be specified in order to propagate $\hat{\mathbf{P}}$ and $\hat{\mathbf{P}}^-$. In practice, these dynamic models will never be known precisely because of the uncertainty in the true nature of the time correlation. As a result, the computed $\hat{\mathbf{P}}$, even using the best dynamic models available, will not accurately describe the probability distribution of the a posteriori estimate error vector. In response, we seek to define a new estimate error covariance matrix $\mathbf{P}$, ($n_x \times n_x$), from which the true estimate error variance σ_y^2 can be upper bounded.

III. Kalman Filtering With Stochastic Modeling Uncertainty

A. A Posteriori Estimate Error Vector

A new derivation of the a posteriori estimate error vector is necessary to observe how $\boldsymbol{\varepsilon}$ is impacted by statistical modeling uncertainty. The derivation begins by revisting the measurement update equation, $\hat{\boldsymbol{x}}_k = \hat{\boldsymbol{x}}_k^- + \mathbf{K}_k(\boldsymbol{z}_k - \mathbf{H}_k\hat{\boldsymbol{x}}_k^-)$. Replacing $\boldsymbol{z}_k$ with the expression on the right hand side of Eq. (1) yields

$$\hat{\boldsymbol{x}}_k = \hat{\boldsymbol{x}}_k^- + \mathbf{K}_k(\mathbf{H}_{\theta,k}\boldsymbol{\theta}_k + \mathbf{J}_{\nu,k}\boldsymbol{\nu}_k - \mathbf{H}_k\hat{\boldsymbol{x}}_k^-). \tag{16}$$

Using the definition $\mathbf{H}_k = [\,\mathbf{H}_{\theta,k} \quad \mathbf{0} \quad \mathbf{J}_{\nu,k}\mathbf{C}_k\,]$ provided after Eq. (11) and writing $\hat{\boldsymbol{x}}_k$ and $\hat{\boldsymbol{x}}_k^-$ in their expanded forms results in

$$\begin{bmatrix}\hat{\boldsymbol{\theta}}_k\\ \hat{\boldsymbol{\xi}}_k\\ \hat{\boldsymbol{\eta}}_k\end{bmatrix} = \begin{bmatrix}\hat{\boldsymbol{\theta}}_k^-\\ \hat{\boldsymbol{\xi}}_k^-\\ \hat{\boldsymbol{\eta}}_k^-\end{bmatrix} - \mathbf{K}_k[\,\mathbf{H}_{\theta,k} \quad \mathbf{0} \quad \mathbf{J}_{\nu,k}\mathbf{C}_k\,]\begin{bmatrix}\hat{\boldsymbol{\theta}}_k^-\\ \hat{\boldsymbol{\xi}}_k^-\\ \hat{\boldsymbol{\eta}}_k^-\end{bmatrix} + \mathbf{K}_k(\mathbf{H}_{\theta,k}\boldsymbol{\theta}_k + \mathbf{J}_{\nu,k}\boldsymbol{\nu}_k) \tag{17}$$

which can be simplified into the form

$$\begin{bmatrix}\hat{\boldsymbol{\theta}}_k\\ \hat{\boldsymbol{\xi}}_k\\ \hat{\boldsymbol{\eta}}_k\end{bmatrix} = \begin{bmatrix}\hat{\boldsymbol{\theta}}_k^-\\ \hat{\boldsymbol{\xi}}_k^-\\ \hat{\boldsymbol{\eta}}_k^-\end{bmatrix} - \mathbf{K}_k\mathbf{H}_k\begin{bmatrix}\hat{\boldsymbol{\theta}}_k^- - \boldsymbol{\theta}_k\\ \hat{\boldsymbol{\xi}}_k^-\\ \hat{\boldsymbol{\eta}}_k^-\end{bmatrix} + \mathbf{K}_k\mathbf{J}_{\nu,k}\boldsymbol{\nu}_k. \tag{18}$$

Subtracting the $n_x \times 1$ vector $[\,\boldsymbol{\theta}_k^T \quad \mathbf{0}^T \quad \mathbf{0}^T\,]^T$ from both sides of Eq. (18) yields

$$\begin{bmatrix}\hat{\boldsymbol{\theta}}_k - \boldsymbol{\theta}_k\\ \hat{\boldsymbol{\xi}}_k\\ \hat{\boldsymbol{\eta}}_k\end{bmatrix} = \begin{bmatrix}\hat{\boldsymbol{\theta}}_k^- - \boldsymbol{\theta}_k\\ \hat{\boldsymbol{\xi}}_k^-\\ \hat{\boldsymbol{\eta}}_k^-\end{bmatrix} - \mathbf{K}_k\mathbf{H}_k\begin{bmatrix}\hat{\boldsymbol{\theta}}_k^- - \boldsymbol{\theta}_k\\ \hat{\boldsymbol{\xi}}_k^-\\ \hat{\boldsymbol{\eta}}_k^-\end{bmatrix} + \mathbf{K}_k\mathbf{J}_{\nu,k}\boldsymbol{\nu}_k. \tag{19}$$

Defining the $n_\theta \times 1$ vectors $\boldsymbol{\varepsilon}_{\theta,k} = \hat{\boldsymbol{\theta}}_k - \boldsymbol{\theta}_k$ and $\boldsymbol{\varepsilon}_{\theta,k}^- = \hat{\boldsymbol{\theta}}_k^- - \boldsymbol{\theta}_k$ allows Eq. (19) to be written as

$$\begin{bmatrix}\boldsymbol{\varepsilon}_{\theta,k}\\ \hat{\boldsymbol{\xi}}_k\\ \hat{\boldsymbol{\eta}}_k\end{bmatrix} = (\mathbf{I} - \mathbf{K}_k\mathbf{H}_k)\begin{bmatrix}\boldsymbol{\varepsilon}_{\theta,k}^-\\ \hat{\boldsymbol{\xi}}_k^-\\ \hat{\boldsymbol{\eta}}_k^-\end{bmatrix} + \mathbf{K}_k\mathbf{J}_{\nu,k}\boldsymbol{\nu}_k. \tag{20}$$

Now define the $n_x \times 1$ vectors $\boldsymbol{e}_k = [\, \boldsymbol{\varepsilon}_{\theta,k}^T \quad \hat{\boldsymbol{\xi}}_k^T \quad \hat{\boldsymbol{\eta}}_k^T \,]^T$ and $\boldsymbol{e}_k^- = [\, \boldsymbol{\varepsilon}_{\theta,k}^{-T} \quad \hat{\boldsymbol{\xi}}_k^{-T} \quad \hat{\boldsymbol{\eta}}_k^{-T} \,]^T$, the $n_x \times n_x$ matrix $\mathbf{L}_k = (\mathbf{I} - \mathbf{K}_k \mathbf{H}_k)$ and the $n_x \times n_\nu$ matrix $\mathbf{M}_k = \mathbf{K}_k \mathbf{J}_{\nu,k}$. Then Eq. (20) can be expressed more succinctly as

$$\boldsymbol{e}_k = \mathbf{L}_k \boldsymbol{e}_k^- + \mathbf{M}_k \boldsymbol{\nu}_k . \tag{21}$$

B. A Priori Estimate Error Vector

A similar procedure can be followed to derive a new expression for the a priori estimate error vector. The derivation begins by writing the time update equation, $\hat{\boldsymbol{x}}_{k+1}^- = \mathbf{F}_k \hat{\boldsymbol{x}}_k$, in the expanded form

$$\begin{bmatrix} \hat{\boldsymbol{\theta}}_{k+1}^- \\ \hat{\boldsymbol{\xi}}_{k+1}^- \\ \hat{\boldsymbol{\eta}}_{k+1}^- \end{bmatrix} = \mathbf{F}_k \begin{bmatrix} \hat{\boldsymbol{\theta}}_k \\ \hat{\boldsymbol{\xi}}_k \\ \hat{\boldsymbol{\eta}}_k \end{bmatrix}. \tag{22}$$

Subtracting the $n_x \times 1$ vector $[\, \boldsymbol{\theta}_{k+1}^T \quad \mathbf{0}^T \quad \mathbf{0}^T \,]^T$ from both sides of Eq. (22) yields

$$\begin{bmatrix} \hat{\boldsymbol{\theta}}_{k+1}^- - \boldsymbol{\theta}_{k+1} \\ \hat{\boldsymbol{\xi}}_{k+1}^- \\ \hat{\boldsymbol{\eta}}_{k+1}^- \end{bmatrix} = \mathbf{F}_k \begin{bmatrix} \hat{\boldsymbol{\theta}}_k \\ \hat{\boldsymbol{\xi}}_k \\ \hat{\boldsymbol{\eta}}_k \end{bmatrix} - \begin{bmatrix} \boldsymbol{\theta}_{k+1} \\ \mathbf{0} \\ \mathbf{0} \end{bmatrix}. \tag{23}$$

From Eq. (2), $\boldsymbol{\theta}_{k+1} = \mathbf{F}_{\theta,k} \boldsymbol{\theta}_k + \mathbf{G}_{\theta,k} \boldsymbol{w}_k$, which can also be written as

$$\begin{bmatrix} \boldsymbol{\theta}_{k+1} \\ \mathbf{0} \\ \mathbf{0} \end{bmatrix} = \begin{bmatrix} \mathbf{F}_{\theta,k} & \mathbf{G}_{\theta,k} \mathbf{A}_k & \mathbf{0} \\ \mathbf{0} & \mathbf{F}_{\xi,k} & \mathbf{0} \\ \mathbf{0} & \mathbf{0} & \mathbf{F}_{\eta,k} \end{bmatrix} \begin{bmatrix} \boldsymbol{\theta}_k \\ \mathbf{0} \\ \mathbf{0} \end{bmatrix} + \begin{bmatrix} \mathbf{G}_{\theta,k} \\ \mathbf{0} \\ \mathbf{0} \end{bmatrix} \boldsymbol{w}_k . \tag{24}$$

The 3×3 block matrix on the right hand side of Eq. (24) is identical to $\mathbf{F}_k$ defined immediately after Eq. (10). Therefore, Eq. (24) can be simplified to

$$\begin{bmatrix} \boldsymbol{\theta}_{k+1} \\ \mathbf{0} \\ \mathbf{0} \end{bmatrix} = \mathbf{F}_k \begin{bmatrix} \boldsymbol{\theta}_k \\ \mathbf{0} \\ \mathbf{0} \end{bmatrix} + \begin{bmatrix} \mathbf{G}_{\theta,k} \\ \mathbf{0} \\ \mathbf{0} \end{bmatrix} \boldsymbol{w}_k . \tag{25}$$

Replacing the vector $[\, \boldsymbol{\theta}_{k+1}^T \quad \mathbf{0}^T \quad \mathbf{0}^T \,]^T$ in Eq. (23) with the right hand side of Eq. (25) and simplifying yields

$$\begin{bmatrix} \hat{\boldsymbol{\theta}}_{k+1}^{-} - \boldsymbol{\theta}_{k+1} \\ \hat{\boldsymbol{\xi}}_{k+1}^{-} \\ \hat{\boldsymbol{\eta}}_{k+1}^{-} \end{bmatrix} = \mathbf{F}_k \begin{bmatrix} \hat{\boldsymbol{\theta}}_k - \boldsymbol{\theta}_k \\ \hat{\boldsymbol{\xi}}_k \\ \hat{\boldsymbol{\eta}}_k \end{bmatrix} - \begin{bmatrix} \mathbf{G}_{\theta,k} \\ \mathbf{0} \\ \mathbf{0} \end{bmatrix} \boldsymbol{w}_k \,. \tag{26}$$

Recalling the definitions of $\boldsymbol{e}_k$ and $\boldsymbol{e}_k^-$ given after Eq. (20), Eq. (26) can also be written as

$$\boldsymbol{e}_{k+1}^- = \mathbf{F}_k \, \boldsymbol{e}_k + \mathbf{N}_k \, \boldsymbol{w}_k \tag{27}$$

where the definition of the $n_x \times n_w$ matrix $\mathbf{N}_k$ is obvious by comparing Eq. (27) to Eq. (26).

Together, Eqs. (21) and (27) constitute a system of linear, time-varying difference equations driven by the actual measurement and process noise sequences. Throughout the derivation above, no assumptions have been made regarding the mathematical structure of the vector time series $\{\boldsymbol{\nu}\}$ and $\{\boldsymbol{w}\}$. Hence, Eqs. (21) and (27) represent the true error in the estimate of the vector $\boldsymbol{\theta}$ after a measurement update and time update of the Kalman filter. The corresponding estimate error covariance matrices $\mathbf{P}_k = E[\boldsymbol{e}_k \, \boldsymbol{e}_k^T]$ and $\mathbf{P}_{k+1}^- = E[\boldsymbol{e}_{k+1}^- \, \boldsymbol{e}_{k+1}^{-T}]$ will be discussed in the next section.

IV. Upper Bounding the Estimate Error Variance

A. A Posteriori Estimate Error Covariance Matrix

In what follows, only $\mathbf{P}_k$ will be considered to illustrate the important aspects of the covariance computation. The same analysis can be carried out for $\mathbf{P}_{k+1}^-$ without difficulty.

From Eq. (21), $\mathbf{P}_k = E[(\mathbf{L}_k \, \boldsymbol{e}_k^- + \mathbf{M}_k \, \boldsymbol{\nu}_k)(\mathbf{L}_k \, \boldsymbol{e}_k^- + \mathbf{M}_k \, \boldsymbol{\nu}_k)^T]$, which expands into the equation

$$\mathbf{P}_k = \mathbf{L}_k \, \mathbf{P}_k^- \, \mathbf{L}_k^T + \mathbf{L}_k \, E[\boldsymbol{e}_k^- \, \boldsymbol{\nu}_k^T] \, \mathbf{M}_k^T + \mathbf{M}_k \, E[\boldsymbol{\nu}_k \, \boldsymbol{e}_k^{-T}] \, \mathbf{L}_k^T + \mathbf{M}_k \, \mathbf{V}_k \, \mathbf{M}_k^T \tag{28}$$

where $\mathbf{V}_k$ is the $n_\nu \times n_\nu$ covariance matrix of $\boldsymbol{\nu}_k$.

The expected values on the right hand side of Eq. (28) are non-zero. To see this, first note that from Eq. (27), $\boldsymbol{e}_k^- = \mathbf{F}_{k-1} \, \boldsymbol{e}_{k-1} + \mathbf{N}_{k-1} \, \boldsymbol{w}_{k-1}$. Replacing $\boldsymbol{e}_{k-1}$ by the expression on the right hand side of Eq. (21) yields

$$\boldsymbol{e}_k^- = \mathbf{F}_{k-1} (\mathbf{L}_{k-1} \, \boldsymbol{e}_{k-1}^- + \mathbf{M}_{k-1} \, \boldsymbol{\nu}_{k-1}) + \mathbf{N}_{k-1} \, \boldsymbol{w}_{k-1} \,. \tag{29}$$

Post-multiplying both sides of Eq. (29) by $\boldsymbol{\nu}_k^T$ and taking the expected value results in

$$E[\mathbf{e}_k^- \boldsymbol{\nu}_k^T] = \mathbf{F}_{k-1}\mathbf{L}_{k-1}E[\mathbf{e}_{k-1}^- \boldsymbol{\nu}_k^T] + \mathbf{F}_{k-1}\mathbf{M}_{k-1}E[\boldsymbol{\nu}_{k-1}\boldsymbol{\nu}_k^T] + \mathbf{N}_{k-1}E[\mathbf{w}_{k-1}\boldsymbol{\nu}_k^T]. \tag{30}$$

Substituting the expression for $\mathbf{e}_{k-1}^-$ from Eq. (29) into the right hand side of Eq. (30) and using the fact that $E[\mathbf{w}_{k-1}\boldsymbol{\nu}_k^T] = \mathbf{0}$ and $E[\mathbf{w}_{k-2}\boldsymbol{\nu}_k^T] = \mathbf{0}$ by virtue of Eq. (5), it can be shown that Eq. (30) becomes

$$\begin{aligned} E[\mathbf{e}_k^- \boldsymbol{\nu}_k^T] = {} & \mathbf{F}_{k-1}\mathbf{L}_{k-1}\mathbf{F}_{k-2}\mathbf{L}_{k-2}E[\mathbf{e}_{k-2}^- \boldsymbol{\nu}_k^T] + \mathbf{F}_{k-1}\mathbf{L}_{k-1}\mathbf{F}_{k-2}\mathbf{M}_{k-2}E[\boldsymbol{\nu}_{k-2}\boldsymbol{\nu}_k^T] \\ & + \mathbf{F}_{k-1}\mathbf{M}_{k-1}E[\boldsymbol{\nu}_{k-1}\boldsymbol{\nu}_k^T] \end{aligned} . \tag{31}$$

Equation (31) can be written in the more compact form

$$E[\mathbf{e}_k^- \boldsymbol{\nu}_k^T] = \mathbf{F}_{k-1}\mathbf{L}_{k-1}\mathbf{F}_{k-2}\mathbf{L}_{k-2}E[\mathbf{e}_{k-2}^- \boldsymbol{\nu}_k^T] + \boldsymbol{\Delta}_2 E[\boldsymbol{\nu}_{k-2}\boldsymbol{\nu}_k^T] + \boldsymbol{\Delta}_1 E[\boldsymbol{\nu}_{k-1}\boldsymbol{\nu}_k^T] \tag{32}$$

where the definitions of $\boldsymbol{\Delta}_1$ ($n_x \times n_\nu$) and $\boldsymbol{\Delta}_2$ ($n_x \times n_\nu$) are obvious by comparing Eq. (32) to Eq. (31).

The process above can be continued, at each step enforcing the fact that $E[\mathbf{w}\boldsymbol{\nu}^T] = \mathbf{0}$, until reaching the conclusion that

$$E[\mathbf{e}_k^- \boldsymbol{\nu}_k^T] = \mathbf{F}_{k-1}\mathbf{L}_{k-1}\mathbf{F}_{k-2}\mathbf{L}_{k-2}\cdots\mathbf{F}_0\mathbf{L}_0 E[\mathbf{e}_0^- \boldsymbol{\nu}_k^T] + \sum_{i=1}^{k} \boldsymbol{\Delta}_i E[\boldsymbol{\nu}_{k-i}\boldsymbol{\nu}_k^T]. \tag{33}$$

Note that because $\mathbf{e}_0^-$ is uncorrelated with $\boldsymbol{\nu}$ at any time, $E[\mathbf{e}_0^- \boldsymbol{\nu}_k^T] = \mathbf{0}$.

The fact that $E[\mathbf{e}_k^- \boldsymbol{\nu}_k^T] \neq \mathbf{0}$ makes it difficult to extract an efficient algorithm for the computation of $\mathbf{P}_k$ and $\mathbf{P}_{k+1}^-$. This issue is addressed in the next section.

B. General Solution to Linear System of Difference Equations

Equations (21) and (27) constitute a set of linear, time-varying difference equations. The solution to any linear system of difference equations can be written in terms of an initial condition response and an impulse response [25].

$$\mathbf{e}_k = \boldsymbol{\Phi}_k \mathbf{e}_0^- + \sum_{\substack{j=1 \\ k \neq 0}}^{n_w} \boldsymbol{\Gamma}_{j,k}\{\mathbf{w}_j\}_0^{k-1} + \sum_{\ell=1}^{n_\nu} \boldsymbol{\Lambda}_{\ell,k}\{\boldsymbol{\nu}_\ell\}_0^k \quad , \quad k \geq 0 \tag{34}$$

$$\boldsymbol{e}_k^- = \boldsymbol{\Phi}_k^- \boldsymbol{e}_0^- + \sum_{\substack{j=1 \\ k\neq 0}}^{n_w} \boldsymbol{\Gamma}_{j,k}^- \{\boldsymbol{w}_j\}_0^{k-1} + \sum_{\substack{\ell=1 \\ k\neq 0}}^{n_v} \boldsymbol{\Lambda}_{\ell,k}^- \{\boldsymbol{v}_\ell\}_0^{k-1} \quad , \quad k \geq 0 \tag{35}$$

where $\boldsymbol{\Phi}_k$ and $\boldsymbol{\Phi}_k^-$ are $n_x \times n_x$ matrices, $\boldsymbol{\Gamma}_{j,k}$ and $\boldsymbol{\Gamma}_{j,k}^-$ are $n_x \times k$ matrices, $\boldsymbol{\Lambda}_{\ell,k}$ is an $n_x \times (k+1)$ matrix, $\boldsymbol{\Lambda}_{\ell,k}^-$ is an $n_x \times k$ matrix, $\{\boldsymbol{w}_j\}_0^{k-1}$ is a $k \times 1$ time series vector for the j^{th} component of $\boldsymbol{w}$ from time index 0 to time index $k-1$ and $\{\boldsymbol{v}_\ell\}_0^{k-1}$ is a $k \times 1$ time series vector for the ℓ^{th} component of $\boldsymbol{v}$ from time index 0 to time index $k-1$.

An algorithm for the computation of $\boldsymbol{\Phi}_k$, $\boldsymbol{\Phi}_k^-$, $\boldsymbol{\Gamma}_{j,k}$, $\boldsymbol{\Gamma}_{j,k}^-$, $\boldsymbol{\Lambda}_{\ell,k}$ and $\boldsymbol{\Lambda}_{\ell,k}^-$ is provided in Appendix A. Evaluating $E[\boldsymbol{e}_k \boldsymbol{e}_k^T]$ and $E[\boldsymbol{e}_k^- \boldsymbol{e}_k^{-T}]$ results in the following expressions for $\mathbf{P}_k$ and $\mathbf{P}_k^-$

$$\mathbf{P}_k = \boldsymbol{\Phi}_k \mathbf{P}_0^- \boldsymbol{\Phi}_k^T + \sum_{\substack{j=1 \\ k\neq 0}}^{n_w} \boldsymbol{\Gamma}_{j,k} \mathbf{W}_{j,k-1} \boldsymbol{\Gamma}_{j,k}^T + \sum_{\ell=1}^{n_v} \boldsymbol{\Lambda}_{\ell,k} \mathbf{V}_{\ell,k} \boldsymbol{\Lambda}_{\ell,k}^T \quad , \quad k \geq 0 \tag{36}$$

$$\mathbf{P}_k^- = \boldsymbol{\Phi}_k^- \mathbf{P}_0^- \boldsymbol{\Phi}_k^{-T} + \sum_{\substack{j=1 \\ k\neq 0}}^{n_w} \boldsymbol{\Gamma}_{j,k}^- \mathbf{W}_{j,k-1} \boldsymbol{\Gamma}_{j,k}^{-T} + \sum_{\substack{\ell=1 \\ k\neq 0}}^{n_v} \boldsymbol{\Lambda}_{\ell,k}^- \mathbf{V}_{\ell,k-1} \boldsymbol{\Lambda}_{\ell,k}^{-T} \quad , \quad k \geq 0 \tag{37}$$

where $\mathbf{P}_0^-$ is the $n_x \times n_x$ covariance matrix $E[\boldsymbol{e}_0^- \boldsymbol{e}_0^{-T}]$, $\mathbf{W}_{j,k-1}$ is the $k \times k$ covariance matrix $E[\{\boldsymbol{w}_j\}_0^{k-1}(\{\boldsymbol{w}_j\}_0^{k-1})^T]$, $\mathbf{V}_{\ell,k}$ is the $(k+1) \times (k+1)$ covariance matrix $E[\{\boldsymbol{v}_\ell\}_0^k(\{\boldsymbol{v}_\ell\}_0^k)^T]$ and $\mathbf{V}_{\ell,k-1}$ is the $k \times k$ covariance matrix $E[\{\boldsymbol{v}_\ell\}_0^{k-1}(\{\boldsymbol{v}_\ell\}_0^{k-1})^T]$.

In this work, the components of $\boldsymbol{v}$ and $\boldsymbol{w}$ are assumed to be wide sense stationary, zero-mean Gaussian random processes. This implies that $\mathbf{W}_{j,k-1}$, $\mathbf{V}_{\ell,k-1}$ and $\mathbf{V}_{\ell,k}$ all have a symmetric Toeplitz structure, for example

$$\mathbf{W}_{j,k-1} = \begin{bmatrix} r_{j,0}^w & r_{j,1}^w & r_{j,2}^w & \cdots & r_{j,k-1}^w \\ r_{j,1}^w & r_{j,0}^w & r_{j,1}^w & \ddots & \vdots \\ r_{j,2}^w & r_{j,1}^w & r_{j,0}^w & \ddots & r_{j,2}^w \\ \vdots & \ddots & \ddots & \ddots & r_{j,1}^w \\ r_{j,k-1}^w & \cdots & r_{j,2}^w & r_{j,1}^w & r_{j,0}^w \end{bmatrix}. \tag{38}$$

The covariance matrix $\mathbf{V}_{\ell,k-1}$ is similar to $\mathbf{W}_{j,k-1}$ except that each $\overset{w}{r}_{j,s}$, $s = 0, \cdots, k-1$ is replaced by $\overset{v}{r}_{\ell,s}$. Furthermore, $\mathbf{V}_{\ell,k}$ is identical to $\mathbf{V}_{\ell,k-1}$ except that the first row and column terminate at $\overset{v}{r}_{\ell,k}$ instead of $\overset{v}{r}_{\ell,k-1}$. A useful feature of the symmetric Toeplitz matrix is that the value along any given diagonal is constant. As a result, it is only necessary to specify the first column of the matrix.

The true estimate error variance of $\varepsilon_{y,k} = \boldsymbol{\alpha}_y^T \boldsymbol{e}_k$ is obtained by applying a covariance transformation to Eq. (36).

$$\sigma_{y,k}^2 = \boldsymbol{\alpha}_y^T \boldsymbol{\Phi}_k \mathbf{P}_0^- \boldsymbol{\Phi}_k^T \boldsymbol{\alpha}_y + \sum_{\substack{j=1 \\ k \neq 0}}^{n_w} \boldsymbol{\alpha}_y^T \boldsymbol{\Gamma}_{j,k} \mathbf{W}_{j,k-1} \boldsymbol{\Gamma}_{j,k}^T \boldsymbol{\alpha}_y + \sum_{\ell=1}^{n_v} \boldsymbol{\alpha}_y^T \boldsymbol{\Lambda}_{\ell,k} \mathbf{V}_{\ell,k} \boldsymbol{\Lambda}_{\ell,k}^T \boldsymbol{\alpha}_y \quad , \quad k \geq 0 . \tag{39}$$

A similar expression for the true a priori variance $\sigma_{y,k}^{-2}$ can be obtained by applying the same covariance transformation to Eq. (37). The second term on the right hand side of Eq. (39) is a sum of quadratic forms in $\mathbf{W}_{j,k-1}$ and the third term is a sum of quadratic forms in $\mathbf{V}_{\ell,k}$. For a general quadratic form $t = \boldsymbol{p}^T \mathbf{A} \boldsymbol{p}$, where $\boldsymbol{p}$ is an $n \times 1$ vector and $\mathbf{A}$ is an $n \times n$ matrix, t can always be expressed as a linear combination of the elements of $\mathbf{A}$. Using this fact, Eq. (39) can be expressed as

$$\sigma_{y,k}^2 = \boldsymbol{\alpha}_y^T \boldsymbol{\Phi}_k \mathbf{P}_0^- \boldsymbol{\Phi}_k^T \boldsymbol{\alpha}_y + \sum_{j=1}^{n_w} \sum_{\substack{s=0 \\ k \neq 0}}^{k-1} \overset{w}{\gamma}_{j,s} \overset{w}{r}_{j,s} + \sum_{\ell=1}^{n_v} \sum_{u=0}^{k} \overset{v}{\gamma}_{\ell,u} \overset{v}{r}_{\ell,u} \quad , \quad k \geq 0 . \tag{40}$$

Expressions for the series coefficients $\overset{w}{\gamma}_{j,s}$ and $\overset{v}{\gamma}_{\ell,u}$ are provided in Appendix B. An analogous expression can be derived for $\sigma_{y,k}^{-2}$ by applying the same procedure to Eq. (37).

C. **Covariance Initialization**

The initial covariance matrix $\mathbf{P}_0^-$ is given by

$$\mathbf{P}_0^- = E\left\{ \begin{bmatrix} \boldsymbol{\varepsilon}_{\theta,0}^- \\ \hat{\boldsymbol{\xi}}_0^- \\ \hat{\boldsymbol{\eta}}_0^- \end{bmatrix} \begin{bmatrix} \boldsymbol{\varepsilon}_{\theta,0}^{-T} & \hat{\boldsymbol{\xi}}_0^{-T} & \hat{\boldsymbol{\eta}}_0^{-T} \end{bmatrix} \right\} = \begin{bmatrix} \mathbf{P}_{\theta,0}^- & \mathbf{0} & \mathbf{0} \\ \mathbf{0} & E[\hat{\boldsymbol{\xi}}_0^- \hat{\boldsymbol{\xi}}_0^{-T}] & \mathbf{0} \\ \mathbf{0} & \mathbf{0} & E[\hat{\boldsymbol{\eta}}_0^- \hat{\boldsymbol{\eta}}_0^{-T}] \end{bmatrix} . \tag{41}$$

The $n_\theta \times n_\theta$ matrix $\mathbf{P}_{\theta,0}^-$ is the covariance matrix of the initial state estimate error vector, $\boldsymbol{\varepsilon}_{\theta,0}^-$. Both $\hat{\boldsymbol{\xi}}_0^-$ and $\hat{\boldsymbol{\eta}}_0^-$ are estimates of the initial state vectors $\boldsymbol{\xi}_0$ and $\boldsymbol{\eta}_0$. Recalling that $\boldsymbol{\xi}$ and $\boldsymbol{\eta}$ were added to model the colored nature of $\boldsymbol{\nu}$ and $\boldsymbol{w}$, respectively, and that $\boldsymbol{\nu}$ and $\boldsymbol{w}$ are zero-mean Gaussian random vectors, it follows that $\hat{\boldsymbol{\xi}}_0^- = \mathbf{0}$ and $\hat{\boldsymbol{\eta}}_0^- = \mathbf{0}$. Furthermore, the initial state estimate is a deterministic vector, which leads to the conclusion that $E[\hat{\boldsymbol{\xi}}_0^- \hat{\boldsymbol{\xi}}_0^{-T}] = \hat{\boldsymbol{\xi}}_0^- \hat{\boldsymbol{\xi}}_0^{-T} = \mathbf{0}$ and $E[\hat{\boldsymbol{\eta}}_0^- \hat{\boldsymbol{\eta}}_0^{-T}] = \hat{\boldsymbol{\eta}}_0^- \hat{\boldsymbol{\eta}}_0^{-T} = \mathbf{0}$. Taking all of these observations into consideration results in an initial estimate error covariance matrix of the form

$$\mathbf{P}_0^- = \begin{bmatrix} \mathbf{P}_{\theta,0}^- & \mathbf{0} & \mathbf{0} \\ \mathbf{0} & \mathbf{0} & \mathbf{0} \\ \mathbf{0} & \mathbf{0} & \mathbf{0} \end{bmatrix}. \tag{42}$$

Equation (40) expresses the true estimate error variance in terms of the autocorrelation function values, $\overset{w}{r}_{j,s}$ and $\overset{\nu}{r}_{\ell,u}$. When the values of $\overset{w}{r}_{j,s}$ and $\overset{\nu}{r}_{\ell,u}$ are precisely known, they are simply inserted into Eq. (40) to compute $\sigma_{y,k}^2$ which is subsequently used to compute the integrity risk. However, in practice the precise values of the autocorrelation functions are most likely unknown which implies that $\sigma_{y,k}^2$ (and consequently the true integrity risk I_y in Eq. (15)) are also unknown. In this case it is necessary to produce a variance $\bar{\sigma}_{y,k}^2$ that upper bounds $\sigma_{y,k}^2$ so that the computed integrity risk $\bar{I}_y$ always upper bounds the true risk. Before the variance bound can be constructed, an uncertainty structure on $\overset{w}{r}_{j,s}$ and $\overset{\nu}{r}_{\ell,u}$ must be specified.

D. Autocorrelation Uncertainty Structure and Associated Variance Bound

In this work, we introduce the bounded uncertainty model

$$\overset{\nu}{a}_{\ell,u} \le \overset{\nu}{r}_{\ell,u} \le \overset{\nu}{b}_{\ell,u} \quad , \quad \ell = 1, \ldots, n_\nu \tag{43}$$

$$\overset{w}{a}_{j,s} \le \overset{w}{r}_{j,s} \le \overset{w}{b}_{j,s} \quad , \quad j = 1, \ldots, n_w \tag{44}$$

Given this uncertainty structure, an upper bound on $\sigma_{y,k}^2$ can be constructed as follows

$$\bar{\sigma}_{y,k}^2 = \boldsymbol{\alpha}_y^T \boldsymbol{\Phi}_k \mathbf{P}_0^- \boldsymbol{\Phi}_k^T \boldsymbol{\alpha}_y + \sum_{j=1}^{n_w} \sum_{\substack{s=0 \\ k \neq 0}}^{k-1} \overset{w}{\gamma}_{j,s} \overset{w}{\bar{r}}_{j,s} + \sum_{\ell=1}^{n_v} \sum_{u=0}^{k} \overset{v}{\gamma}_{\ell,u} \overset{v}{\bar{r}}_{\ell,u} \quad , \quad k \geq 0 \tag{45}$$

where $\bar{\sigma}_{y,k}^2$ is the variance upper bound and $\overset{w}{\bar{r}}_{j,s}$ and $\overset{v}{\bar{r}}_{\ell,u}$ are defined as

$$\overset{w}{\bar{r}}_{j,s} = \begin{cases} \overset{w}{a}_{j,s} & , \quad \overset{w}{\gamma}_{j,s} < 0 \\ \overset{w}{b}_{j,s} & , \quad \overset{w}{\gamma}_{j,s} \geq 0 \end{cases} \quad \text{and} \quad \overset{v}{\bar{r}}_{\ell,u} = \begin{cases} \overset{v}{a}_{\ell,u} & , \quad \overset{v}{\gamma}_{\ell,u} < 0 \\ \overset{v}{b}_{\ell,u} & , \quad \overset{v}{\gamma}_{\ell,u} \geq 0 \end{cases} . \tag{46}$$

V. One-Dimensional Position and Velocity Estimation

The algorithms developed above will now be applied to the estimation problem shown in Fig. 1.

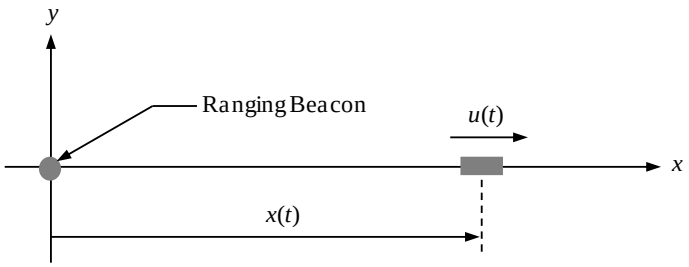

Fig. 1: One-dimensional estimation problem.

The position $x(t)$ and velocity $u(t)$ along the *x*-axis are estimated using an accelerometer attached to the vehicle and a ranging beacon located at the origin. Assume that the *x*-*y* coordinate system is horizontal and constitutes an inertial reference frame.

The measurement model for the ranging beacon is given by $z_k = x_k + \nu_k$, where z_k is the measurement at time index *k*, x_k is the position of the vehicle at time index *k* and ν_k is the measurement noise at time index *k*.

The continuous–time dynamic model for the vehicle position and velocity are given by

$$\dot{x}(t) = u(t) \tag{47}$$

$$\dot{u}(t) = a(t) \tag{48}$$

where $a(t)$ is a scalar function representing the vehicle's inertial acceleration along the x-axis.

During operation, the accelerometer outputs the integral of a signal $\tilde{a}(t)$ that is the sum of the vehicle acceleration and any random disturbances that are present. That is, $\tilde{a}(t) = a(t) + \beta(t)$, where $\beta(t)$ is a random disturbance input. Using this relation, the velocity dynamic model in Eq. (48) can also be written as

$$\dot{u}(t) = \tilde{a}(t) - \beta(t) . \tag{49}$$

In order to use a Kalman filter to estimate x and u, Eqs. (47) and (49) must be converted to a set of discrete-time equations. Integrating both sides of Eq. (49) from time index *k* to time index *k* + 1 yields

$$u_{k+1} = u_k + \int_k^{k+1} [\, \tilde{a}(\tau) - \beta(\tau) \,] d\tau . \tag{50}$$

Making the definitions $\Delta u_k = \int_k^{k+1} \tilde{a}(\tau)\, d\tau$ and $w_k = \int_k^{k+1} \beta(\tau)\, d\tau$ allows Eq. (50) to be written in the form $u_{k+1} = u_k + \Delta u_k - w_k$, where Δu_k is the accelerometer measurement and w_k is the associated accelerometer measurement noise.

A similar procedure can be followed to convert Eq. (47) to discrete-time form. Integrating both sides of Eq. (47) from time index *k* to time index *k* + 1 results in

$$x_{k+1} = x_k + \int_k^{k+1} u(\tau)\, d\tau . \tag{51}$$

In order to perform the integration, a functional expression for $u(t)$ is required. Assuming that $a(t)$ is approximately constant over the integration interval allows Eq. (48) to be written as $u(t) \approx u_k + a(t - t_k)$, $t \in [t_k , t_{k+1}]$. Inserting this expression into Eq. (51) and performing the integration yields

$$x_{k+1} = x_k + u_k \Delta t + \frac{1}{2} a \Delta t^2 \quad , \quad \Delta t = t_{k+1} - t_k . \tag{52}$$

The acceleration over the interval $[t_k , t_{k+1}]$ is approximately equal to $(u_{k+1} - u_k) / \Delta t$. Substituting the expression $u_{k+1} = u_k + \Delta u_k - w_k$ provided after Eq. (50) results in $a \approx (\Delta u_k - w_k) / \Delta t$. Substituting this relation into Eq. (52) yields the discrete−time position dynamic model

$$x_{k+1} = x_k + u_k \Delta t + \frac{\Delta t}{2} \Delta u_k - \frac{\Delta t}{2} w_k . \tag{53}$$

When taken together, the position and velocity dynamic models can be written in the state space form

$$\begin{bmatrix} x_{k+1} \\ u_{k+1} \end{bmatrix} = \begin{bmatrix} 1 & \Delta t \\ 0 & 1 \end{bmatrix} \begin{bmatrix} x_k \\ u_k \end{bmatrix} + \begin{bmatrix} \Delta t / 2 \\ 1 \end{bmatrix} \Delta u_k - \begin{bmatrix} \Delta t / 2 \\ 1 \end{bmatrix} w_k \tag{54}$$

which can finally be expressed as $\boldsymbol{\theta}_{k+1} = \mathbf{F}_{\theta,k} \boldsymbol{\theta}_k + \mathbf{G}_{u,k} \Delta u_k + \mathbf{G}_{\theta,k} w_k$. Notice that this expression is slightly different from the linear dynamic model given in Eq. (2) due to the presence of the term $\mathbf{G}_{u,k} \Delta u_k$. However, this vector is entirely known and therefore its presence does not impact the estimate error covariance matrix. Also note that no modification of the ranging beacon measurement equation, $z_k = x_k + \nu_k$, is required. It is already in the form of Eq. (1) with $\mathbf{H}_{\theta,k} = [1 \quad 0]$ and $\mathbf{J}_{\nu,k} = 1$.

For this example, the ranging beacon measurement noise ν_k can be decomposed as $\nu_k = \eta_k + r_k$, where $\{r\}$ is a zero-mean, white Gaussian noise process with variance σ_r^2 and $\{\eta\}$ is a first order Gauss-Markov process. The continuous time dynamic model of η is given by

$$\dot{\eta}(t) = -\frac{1}{\tau_\eta} \eta(t) + q_\eta(t) \quad , \quad \eta(0) \sim N(0 \, , \sigma_\eta^2) \tag{55}$$

where τ_η is the time constant of the Gauss-Markov process, σ_η^2 is the variance of the Gauss-Markov process and $\{q_\eta\}$ is a zero-mean, white Gaussian noise process with power spectral density $Q_\eta = 2\sigma_\eta^2 / \tau_\eta$.

Similarly, the disturbance input $\beta(t)$ can be decomposed as $\beta(t) = \xi(t) + q_\theta(t)$, where $\{q_\theta\}$ is a zero-mean, white Gaussian noise process with power spectral density Q_θ and $\{\xi\}$ is a first-order Gauss-Markov process governed by the dynamic model

$$\dot{\xi}(t) = -\frac{1}{\tau_\xi} \xi(t) + q_\xi(t) \quad , \quad \xi(0) \sim N(0 \, , \sigma_\xi^2) \tag{56}$$

where τ_ξ is the time constant of the Gauss-Markov process, σ_ξ^2 is the variance of the Gauss-Markov process and $\{q_\xi\}$ is a zero-mean, white Gaussian noise process with power spectral density $Q_\xi = 2\sigma_\xi^2 / \tau_\xi$.

Collecting Eqs. (47), (49), (55) and (56) into one matrix-vector equation results in the state-augmented dynamic model

$$\begin{bmatrix} \dot{x}(t) \\ \dot{u}(t) \\ \dot{\xi}(t) \\ \dot{\eta}(t) \end{bmatrix} = \begin{bmatrix} 0 & 1 & 0 & 0 \\ 0 & 0 & -1 & 0 \\ 0 & 0 & -1/\tau_\xi & 0 \\ 0 & 0 & 0 & -1/\tau_\eta \end{bmatrix} \begin{bmatrix} x(t) \\ u(t) \\ \xi(t) \\ \eta(t) \end{bmatrix} + \begin{bmatrix} 0 \\ 1 \\ 0 \\ 0 \end{bmatrix} \tilde{a}(t) + \begin{bmatrix} 0 & 0 & 0 \\ -1 & 0 & 0 \\ 0 & 1 & 0 \\ 0 & 0 & 1 \end{bmatrix} \begin{bmatrix} q_\theta(t) \\ q_\xi(t) \\ q_\eta(t) \end{bmatrix} \tag{57}$$

where the substitution $\beta(t) = \xi(t) + q_\theta(t)$ has been made in Eq. (49).

Well known methods exist to convert Eq. (57) to the discrete-time form $\boldsymbol{x}_{k+1} = \mathbf{F}_k \boldsymbol{x}_k + \mathbf{G}_{u,k} \Delta u_k + \boldsymbol{q}_k$ and expressions for $\mathbf{F}_k$ and $\mathbf{G}_{u,k}$ can be found in [26]. The covariance matrix of $\boldsymbol{q}_k$ is determined using the Van Loan algorithm [27].

It is important to reiterate that in a real estimation application, the mathematical models used in the state-augmentation process are not the true mathematical models of the measurement and process noise. In this example, however, it is assumed that the beacon measurement noise and accelerometer measurement noise really are the sum of a white Gaussian noise process and a first order Gauss-Markov process. The parameters defining these models are only known to lie between the intervals specified in Table 1.

Table 1 Specified ranges on sensor noise characteristics

Accelerometer	Ranging Beacon
$\sqrt{Q_\theta} \in [5\ ,\ 10]\ \mu g/\sqrt{Hz}$	$\sigma_r \in [0.25\ ,\ 0.5]$ m
$\sigma_\xi \in [30\ ,\ 50]\ \mu g$	$\sigma_\eta \in [0.75\ ,\ 1.0]$ m
$\tau_\xi \in [50\ ,\ 75]$ sec	$\tau_\eta \in [40\ ,\ 60]$ sec

In order to use the bounding algorithm specified in Eqs. (45) and (46), upper and lower autocorrelation bounding functions on $\overset{w}{r}_{j,s}$ and $\overset{v}{r}_{\ell,u}$ must be defined. Given that the measurement and process noise variables v and w are scalars for this example the indices j and ℓ can only take on a value of 1, and therefore $\overset{w}{r}_{j,s}$ and $\overset{v}{r}_{\ell,u}$ will be replaced by $\overset{w}{r}_{1,s}$ and $\overset{v}{r}_{1,u}$, respectively. It is shown in Appendix C that the autocorrelation function of w is given by

$$\overset{w}{r}_{1,s} = \begin{cases} 2(\sigma_\xi \tau_\xi)^2 \left[\dfrac{\Delta t}{\tau_\xi} - 1 + \exp\left(-\dfrac{\Delta t}{\tau_\xi} \right) \right] + Q_\theta \, \Delta t & , \quad s = 0 \\ (\sigma_\xi \tau_\xi)^2 \exp\left(-\dfrac{|s\Delta t|}{\tau_\xi} \right) \left[1 - \exp\left(-\dfrac{\Delta t}{\tau_\xi} \right) \right] \left[\exp\left(\dfrac{\Delta t}{\tau_\xi} \right) - 1 \right] & , \quad s \neq 0 \end{cases} \tag{58}$$

where *s* can only take on integer values.

The autocorrelation function of ν is more straightforward. For the Gauss-Markov component of the beacon measurement noise, the autocorrelation function is given by [28]

$$\overset{\eta}{r}_{1,u} = \sigma_\eta^2 \exp\left(-\frac{|u\Delta t|}{\tau_\eta} \right) \tag{59}$$

where *u* is an integer that should not be confused with the vehicle velocity.

The white noise component of ν has an autocorrelation function defined by

$$\overset{r}{r}_{1,u} = \begin{cases} \sigma_r^2 & , \quad u = 0 \\ 0 & , \quad u \neq 0 \end{cases}. \tag{60}$$

When Eqs. (59) and (60) are combined, the autocorrelation function of ν is described by the equation

$$\overset{\nu}{r}_{1,u} = \begin{cases} \sigma_\eta^2 + \sigma_r^2 & , \quad u = 0 \\ \sigma_\eta^2 \exp\left(-\dfrac{|u\Delta t|}{\tau_\eta} \right) & , \quad u \neq 0 \end{cases}. \tag{61}$$

The upper and lower bounding functions on $\overset{w}{r}_{1,s}$ and $\overset{\nu}{r}_{1,u}$ are obtained by substituting the upper and lower bounding values from Table 1 into Eqs. (58) and (61). Design values of τ_ξ, τ_η, σ_ξ^2, σ_η^2, Q_θ and σ_r^2 must be specified in order to define the Kalman filter. Designers typically choose the maximum variance (or power spectral density) and time constant to define the filter. In this work, the same approach is adopted and the filter is defined using the upper bound values in Table 1. The rationale behind this choice is that measurements with highly correlated errors do not provide as much new information as measurements whose errors are less correlated. This in turn should produce a larger estimate error variance. However, it will be shown shortly that these qualitative arguments do not always work.

The last step to complete before conducting the simulation is to specify the Kalman filter initial covariance matrix, $\hat{\mathbf{P}}_0^-$, and the bounding algorithm initial covariance matrix, $\mathbf{P}_0^-$. For this example, $\hat{\mathbf{P}}_0^-$ is set equal to

$$\hat{\mathbf{P}}_0^- = \begin{bmatrix} (10\text{ m})^2 & 0 & 0 & 0 \\ 0 & (1\text{ m/s})^2 & 0 & 0 \\ 0 & 0 & (50\ \mu\text{g})^2 & 0 \\ 0 & 0 & 0 & (1\text{ m})^2 \end{bmatrix}. \tag{62}$$

Recall from Eq. (42) that the only non-zero elements of $\mathbf{P}_0^-$ are those that belong to the upper left $n_\theta \times n_\theta$ matrix which in turn are identical to the values in the upper left $n_\theta \times n_\theta$ matrix of $\hat{\mathbf{P}}_0^-$. Given that $n_\theta = 2$, this results in the following form for $\mathbf{P}_0^-$

$$\mathbf{P}_0^- = \begin{bmatrix} (10\text{ m})^2 & 0 & 0 & 0 \\ 0 & (1\text{ m/s})^2 & 0 & 0 \\ 0 & 0 & 0 & 0 \\ 0 & 0 & 0 & 0 \end{bmatrix}. \tag{63}$$

A truth model for the ranging beacon and accelerometer error autocorrelation functions is required to ascertain the tightness of the variance bound. The parameters defining this model are summarized in Table 2.

Table 2 True sensor noise characteristics

Accelerometer	Ranging Beacon
$\sqrt{Q_\theta} = 10\ \mu\text{g}/\sqrt{\text{Hz}}$	$\sigma_r = 0.5$ m
$\sigma_\xi = 50\ \mu\text{g}$	$\sigma_\eta = 1.0$ m
$\tau_\xi = 62.5$ sec	$\tau_\eta = 50$ sec

The values from Table 2 are substituted into Eqs. (58) and (61) to determine the true correlation functions $\overset{w}{r}_{1,s}$ and $\overset{v}{r}_{1,u}$, which are subsequently inserted into Eq. (40) to compute the true estimate error variance, σ_y^2.

The ranging beacon and accelerometer measurement sampling intervals are equal to 5 sec (i.e. $\Delta t = 5\,\text{sec}$). A total of 60 measurement epochs are simulated, for a total simulation time scale of 300 seconds. In this case, the autocorrelation bounding functions and the assumed truth models can be represented graphically in Figs. 2 and 3.

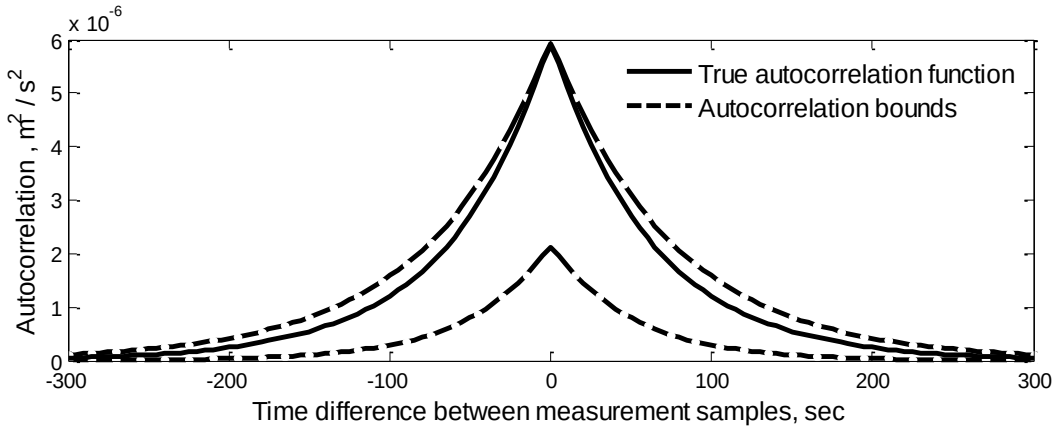

Fig. 2: Bounds on accelerometer error autocorrelation function with truth model.

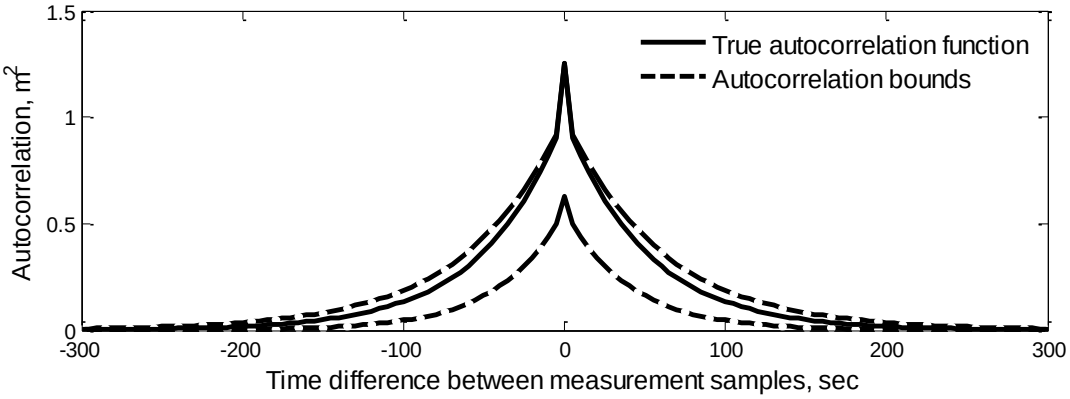

Fig. 3: Bounds on ranging beacon error autocorrelation function with truth model.

For the position state, there are three variances of interest: the position estimate error variance output from the Kalman filter, the true position estimate error variance and the bounding position estimate error variance. Each of these variances is denoted by $\hat{\sigma}_x^2$, σ_x^2 and $\bar{\sigma}_x^2$, respectively, and are obtained from $\hat{\mathbf{P}}$ and $\mathbf{P}$ accordingly using the coefficient vector $\boldsymbol{\alpha}_x = [\,1 \quad 0 \quad 0 \quad 0\,]^T$. Since the a posteriori state estimate is the best available estimate at any given time index, only the posterior estimate error variances will be shown.

Figure 4 shows a plot of the difference $\bar{\sigma}_x - \sigma_x$ versus elapsed time. This difference is always a positive number, indicating that the bounding variance $\bar{\sigma}_x^2$ always upper bounds the true variance, σ_x^2. It is also interesting to see whether or not the heuristics used to define the estimator produce a filter variance that also upper bounds the

true variance. Figure 5 shows a plot of $\hat{\sigma}_x - \sigma_x$ versus elapsed time. Between 0 seconds and approximately 35 seconds this difference is negative, suggesting that $\hat{\sigma}_x^2$ does not upper bound σ_x^2 in this region. Therefore, the intuitive approach of basing the filter models on the maximum measurement error variance and time constant does not guarantee that $\hat{\sigma}_x^2$ will always upper bound σ_x^2.

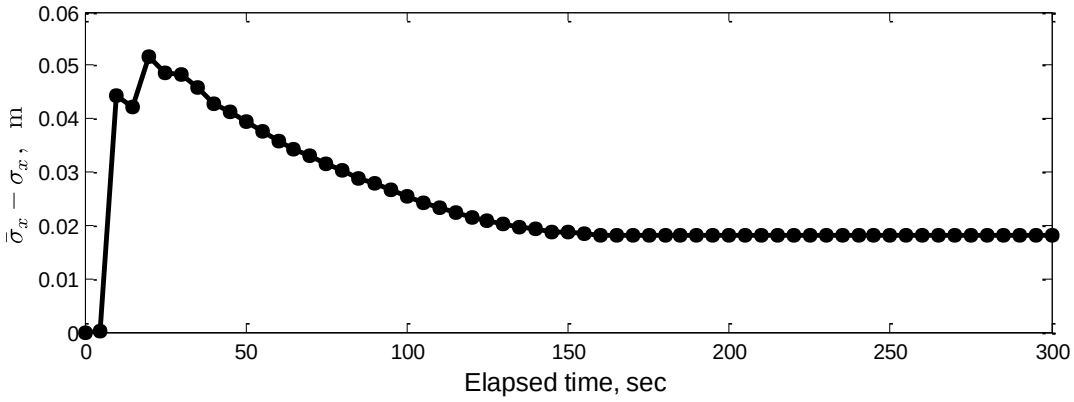

Fig. 4: Difference between bounded and true standard deviations of the position estimate error.

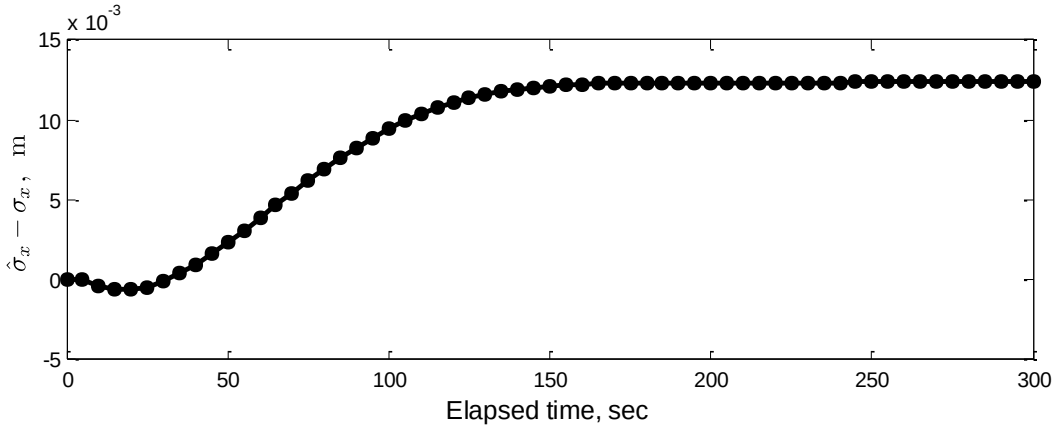

Fig. 5: Difference between filter and true standard deviations of the position estimate error.

For each point plotted in Fig. 4 there is a corresponding accelerometer autocorrelation function $\overset{w}{\bar{r}}_{1,s}$ and a beacon autocorrelation function $\overset{v}{\bar{r}}_{1,u}$ that created $\bar{\sigma}_x^2$. To illustrate the nature of $\overset{w}{\bar{r}}_{1,s}$ and $\overset{v}{\bar{r}}_{1,u}$, consider the final filtering point at an elapsed time of 300 sec. From Fig. 6 it can be seen that $\overset{v}{\bar{r}}_{1,u}$ begins at the upper bounding

function and then drops sharply to the lower bounding function after approximately 75 seconds of filtering. The accelerometer autocorrelation function displays similar behavior. Figure 7 shows that $\bar{r}^{w}_{1,s}$ also begins at the upper bounding function and then suddenly drops to the lower bounding function after approximately 120 seconds of filtering.

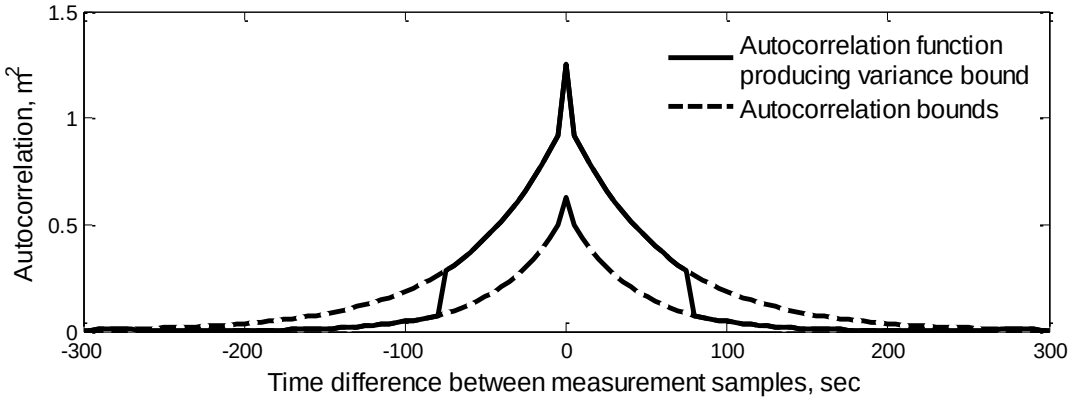

Fig. 6: Beacon error autocorrelation function corresponding to upper bounding position estimate error variance.

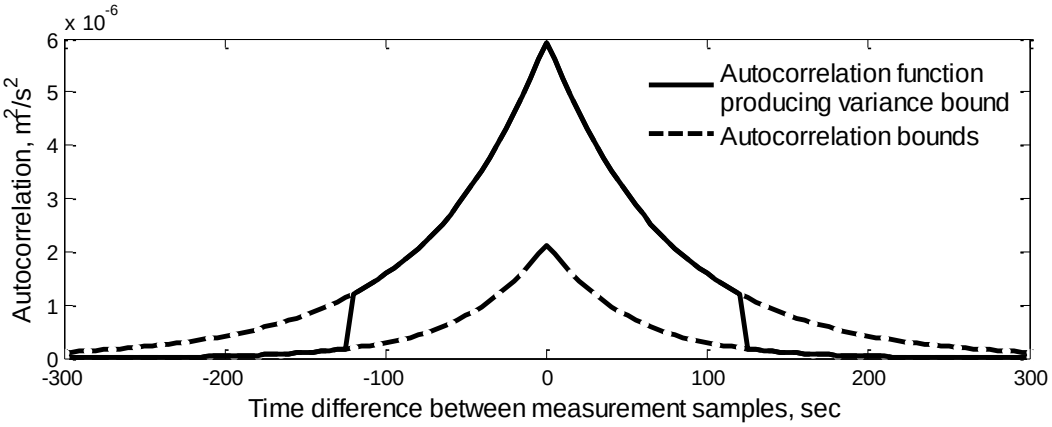

Fig. 7: Accelerometer error autocorrelation function corresponding to upper bounding position estimate error variance.

A similar analysis can be conducted for the velocity state by using the coefficient vector $\boldsymbol{\alpha}_u = [\,0 \quad 1 \quad 0 \quad 0\,]^T$. An important aspect of the bounding method proposed in this work is that the variance upper bound must be computed separately for each element of the state vector that requires a bound.

The autocorrelation functions shown in Figs. 6 and 7 that produce the variance bound have interesting ramifications. Recall that $\overset{w}{r}_{1,s}$ and $\overset{v}{r}_{1,u}$ ultimately determine the covariance matrices $\mathbf{W}$ and $\mathbf{V}$ in Eq. (39), which should always be positive semi-definite. However, when $\overset{w}{\bar{r}}_{1,s}$ and $\overset{v}{\bar{r}}_{1,u}$ are used to populate $\mathbf{W}$ and $\mathbf{V}$, it can be shown that $\mathbf{W}$ and $\mathbf{V}$ are not positive semi-definite, which implies that the upper bound $\bar{\sigma}_x^2$ may be unnecessarily conservative. Imposing a positive semi-definiteness constraint on $\mathbf{W}$ and $\mathbf{V}$ could significantly reduce the upper bound $\bar{\sigma}_x^2$, thereby tightening the integrity risk upper bound. However, this requires formulating an optimization problem that would need to be solved via semi-definite programming. This approach will be pursued in future advancements of this research.

VI. Conclusion

In this paper, a new method was developed to upper bound integrity risk for sequential state estimators subject to stochastic modeling uncertainty. Using a new derivation of the Kalman state estimate error vector, it was shown how this upper bound can be computed subject to a bounded autocorrelation uncertainty structure. The method was demonstrated for a one dimensional position and velocity estimation problem, and it was shown that often-used heuristic arguments do not provide an upper bound on integrity risk. Therefore, the method developed in this paper provides a direct means to ensure integrity in safety critical estimation applications in the presence of disturbance and sensor noise stochastic modeling uncertainty.

Appendix A

This appendix derives the general solution to the following system of linear difference equations

$$\boldsymbol{e}_k = \mathbf{L}_k \boldsymbol{e}_k^- + \mathbf{M}_k \boldsymbol{\nu}_k \quad , \quad k \geq 0 \tag{1A}$$

$$\boldsymbol{e}_{k+1}^- = \mathbf{F}_k \boldsymbol{e}_k + \mathbf{N}_k \boldsymbol{w}_k \quad , \quad k \geq 0 \tag{2A}$$

where $\boldsymbol{e}_k$, $\boldsymbol{e}_k^-$ and $\boldsymbol{e}_{k+1}^-$ are $n_x \times 1$ vectors, $\mathbf{L}_k$ is an $n_x \times n_x$ matrix, $\mathbf{M}_k$ is an $n_x \times n_\nu$ matrix, $\boldsymbol{\nu}_k$ is an $n_\nu \times 1$ vector, $\mathbf{F}_k$ is an $n_x \times n_x$ matrix, $\mathbf{N}_k$ is an $n_x \times n_w$ matrix and $\boldsymbol{w}_k$ is an $n_w \times 1$ vector.

When $k = 0$, Eq. (1A) can be written in the form

$$\boldsymbol{e}_0 = \boldsymbol{\Phi}_0 \boldsymbol{e}_0^- + \sum_{\ell=1}^{n_\nu} \boldsymbol{\Lambda}_{\ell,0} \nu_{\ell,0} \tag{3A}$$

where $\boldsymbol{\Phi}_0 = \mathbf{L}_0$, $\boldsymbol{\Lambda}_{\ell,0}$ is an $n_x \times 1$ vector equal to the ℓ^{th} column of $\mathbf{M}_0$ (i.e. $\boldsymbol{\Lambda}_{\ell,0} = \mathbf{M}_0(:, \ell)$) and $\nu_{\ell,0}$ is a scalar corresponding to the ℓ^{th} component of $\boldsymbol{\nu}_0$.

Similarly, when k = 0, Eq. (2A) can be written as $\boldsymbol{e}_1^- = \mathbf{F}_0 \boldsymbol{e}_0 + \sum_{j=1}^{n_w} \mathbf{N}_0(:, j) w_{j,0}$, where $\mathbf{N}_0(:, j)$ is an $n_x \times 1$ vector corresponding to the j^{th} column of $\mathbf{N}_0$ and $w_{j,0}$ is a scalar corresponding to the j^{th} component of $\boldsymbol{w}_0$. Replacing $\boldsymbol{e}_0$ by the expression on the right hand side of Eq. (3A) results in

$$\boldsymbol{e}_1^- = \mathbf{F}_0 \boldsymbol{\Phi}_0 \boldsymbol{e}_0^- + \sum_{\ell=1}^{n_\nu} \mathbf{F}_0 \boldsymbol{\Lambda}_{\ell,0} \nu_{\ell,0} + \sum_{j=1}^{n_w} \mathbf{N}_0(:, j) w_{j,0}. \tag{4A}$$

Defining the $n_x \times n_x$ matrix $\boldsymbol{\Phi}_1^- = \mathbf{F}_0 \boldsymbol{\Phi}_0$, the $n_x \times 1$ vector $\boldsymbol{\Lambda}_{\ell,1}^- = \mathbf{F}_0 \boldsymbol{\Lambda}_{\ell,0}$ and the $n_x \times 1$ vector $\boldsymbol{\Gamma}_{j,1}^- = \mathbf{N}_0(:, j)$ allows Eq. (4A) to be expressed more compactly as

$$\boldsymbol{e}_1^- = \boldsymbol{\Phi}_1^- \boldsymbol{e}_0^- + \sum_{\ell=1}^{n_\nu} \boldsymbol{\Lambda}_{\ell,1}^- \nu_{\ell,0} + \sum_{j=1}^{n_w} \boldsymbol{\Gamma}_{j,1}^- w_{j,0}. \tag{5A}$$

When k = 1, Eq. (1A) becomes $\boldsymbol{e}_1 = \mathbf{L}_1 \boldsymbol{e}_1^- + \sum_{\ell=1}^{n_\nu} \mathbf{M}_1(:, \ell) \nu_{\ell,1}$, where $\mathbf{M}_1(:, \ell)$ is an $n_x \times 1$ vector corresponding to the ℓ^{th} column of $\mathbf{M}_1$ and $\nu_{\ell,1}$ is a scalar corresponding to the ℓ^{th} component of $\boldsymbol{\nu}_1$. Replacing $\boldsymbol{e}_1^-$ by the expression on the right hand side of Eq. (5A) results in

$$\boldsymbol{e}_1 = \mathbf{L}_1 \boldsymbol{\Phi}_1^- \boldsymbol{e}_0^- + \sum_{\ell=1}^{n_\nu} \mathbf{L}_1 \boldsymbol{\Lambda}_{\ell,1}^- \nu_{\ell,0} + \sum_{j=1}^{n_w} \mathbf{L}_1 \boldsymbol{\Gamma}_{j,1}^- w_{j,0} + \sum_{\ell=1}^{n_\nu} \mathbf{M}_1(:, \ell) \nu_{\ell,1}. \tag{6A}$$

Defining the $n_x \times n_x$ matrix $\boldsymbol{\Phi}_1 = \mathbf{L}_1 \boldsymbol{\Phi}_1^-$, the $n_x \times 2$ matrix $\boldsymbol{\Lambda}_{\ell,1} = [\, \mathbf{L}_1 \boldsymbol{\Lambda}_{\ell,1}^- \,|\, \mathbf{M}_1(:, \ell) \,]$, the $n_x \times 1$ vector $\boldsymbol{\Gamma}_{j,1} = \mathbf{L}_1 \boldsymbol{\Gamma}_{j,1}^-$ and the 2×1 vector $\{\boldsymbol{\nu}_\ell\}_0^1 = [\, \nu_{\ell,0} \quad \nu_{\ell,1} \,]^T$ allows Eq. (6A) to be expressed more compactly as

$$\boldsymbol{e}_1 = \boldsymbol{\Phi}_1 \boldsymbol{e}_0^- + \sum_{\ell=1}^{n_\nu} \boldsymbol{\Lambda}_{\ell,1} \{\boldsymbol{\nu}_\ell\}_0^1 + \sum_{j=1}^{n_w} \boldsymbol{\Gamma}_{j,1} w_{j,0}. \tag{7A}$$

Similarly, when k = 1, Eq. (2A) becomes $\boldsymbol{e}_2^- = \mathbf{F}_1 \boldsymbol{e}_1 + \sum_{j=1}^{n_w} \mathbf{N}_1(:, j)\, w_{j,1}$, where $\mathbf{N}_1(:, j)$ is an $n_x \times 1$ vector corresponding to the j^{th} column of $\mathbf{N}_1$ and $w_{j,1}$ is a scalar corresponding to the j^{th} component of $\boldsymbol{w}_1$. Replacing $\boldsymbol{e}_1$ by the expression on the right hand side of Eq. (7A) results in

$$\boldsymbol{e}_2^- = \mathbf{F}_1 \boldsymbol{\Phi}_1 \boldsymbol{e}_0^- + \sum_{\ell=1}^{n_v} \mathbf{F}_1 \boldsymbol{\Lambda}_{\ell,1} \{\boldsymbol{\nu}_\ell\}_0^1 + \sum_{j=1}^{n_w} \mathbf{F}_1 \boldsymbol{\Gamma}_{j,1}\, w_{j,0} + \sum_{j=1}^{n_w} \mathbf{N}_1(:, j)\, w_{j,1}. \tag{8A}$$

Defining the $n_x \times n_x$ matrix $\boldsymbol{\Phi}_2^- = \mathbf{F}_1 \boldsymbol{\Phi}_1$, the $n_x \times 2$ matrix $\boldsymbol{\Lambda}_{\ell,2}^- = \mathbf{F}_1 \boldsymbol{\Lambda}_{\ell,1}$, the $n_x \times 2$ matrix $\boldsymbol{\Gamma}_{j,2}^- = [\, \mathbf{F}_1 \boldsymbol{\Gamma}_{j,1} \,|\, \mathbf{N}_1(:, j) \,]$ and the 2×1 vector $\{\boldsymbol{w}_j\}_0^1 = [\, w_{j,0} \quad w_{j,1} \,]^T$ allows Eq. (8A) to be expressed more compactly as

$$\boldsymbol{e}_2^- = \boldsymbol{\Phi}_2^- \boldsymbol{e}_0^- + \sum_{\ell=1}^{n_v} \boldsymbol{\Lambda}_{\ell,2}^- \{\boldsymbol{\nu}_\ell\}_0^1 + \sum_{j=1}^{n_w} \boldsymbol{\Gamma}_{j,2}^- \{\boldsymbol{w}_j\}_0^1. \tag{9A}$$

This process can be continued, resulting in the expressions

$$\boldsymbol{e}_k = \boldsymbol{\Phi}_k \boldsymbol{e}_0^- + \sum_{\substack{j=1 \\ k \neq 0}}^{n_w} \boldsymbol{\Gamma}_{j,k} \{\boldsymbol{w}_j\}_0^{k-1} + \sum_{\ell=1}^{n_v} \boldsymbol{\Lambda}_{\ell,k} \{\boldsymbol{\nu}_\ell\}_0^k \quad , \quad k \geq 0 \tag{10A}$$

$$\boldsymbol{e}_k^- = \boldsymbol{\Phi}_k^- \boldsymbol{e}_0^- + \sum_{\substack{j=1 \\ k \neq 0}}^{n_w} \boldsymbol{\Gamma}_{j,k}^- \{\boldsymbol{w}_j\}_0^{k-1} + \sum_{\substack{\ell=1 \\ k \neq 0}}^{n_v} \boldsymbol{\Lambda}_{\ell,k}^- \{\boldsymbol{\nu}_\ell\}_0^{k-1} \quad , \quad k \geq 0 \tag{11A}$$

where $\boldsymbol{\Phi}_k$ and $\boldsymbol{\Phi}_k^-$ are $n_x \times n_x$ matrices, $\boldsymbol{\Gamma}_{j,k}$ and $\boldsymbol{\Gamma}_{j,k}^-$ are $n_x \times k$ matrices, $\boldsymbol{\Lambda}_{\ell,k}$ is an $n_x \times (k + 1)$ matrix, $\boldsymbol{\Lambda}_{\ell,k}^-$ is an $n_x \times k$ matrix, $\{\boldsymbol{w}_j\}_0^{k-1}$ is a $k \times 1$ time series vector for the j^{th} component of $\boldsymbol{w}$ from time index 0 to time index $k - 1$, $\{\boldsymbol{\nu}_\ell\}_0^{k-1}$ is a $k \times 1$ time series vector for the ℓ^{th} component of $\boldsymbol{\nu}$ from time index 0 to time index $k - 1$ and $\{\boldsymbol{\nu}_\ell\}_0^k$ is a $(k + 1) \times 1$ time series vector for the ℓ^{th} component of $\boldsymbol{\nu}$ from time index 0 to time index k.

The matrices in Eqs. (10A) and (11A) are defined as

$$\boldsymbol{\Phi}_k = \mathbf{L}_k \boldsymbol{\Phi}_k^- \quad , \quad k \geq 0 \quad , \quad \boldsymbol{\Phi}_0^- = \mathbf{I} \tag{12A}$$

$$\boldsymbol{\Lambda}_{\ell,k} = [\, \mathbf{L}_k \, \boldsymbol{\Lambda}^{-}_{\ell,k} \,|\, \mathbf{M}_k \,(:,\, \ell\,)\,] \quad , \quad k \geq 0 \quad , \quad \boldsymbol{\Lambda}^{-}_{\ell,0} = [\,] \tag{13A}$$

$$\boldsymbol{\Gamma}_{j,k} = \mathbf{L}_k \, \boldsymbol{\Gamma}^{-}_{j,k} \quad , \quad k > 0 \tag{14A}$$

$$\boldsymbol{\Phi}^{-}_{k} = \mathbf{F}_{k-1} \, \boldsymbol{\Phi}_{k-1} \quad , \quad k \geq 0 \quad , \quad \boldsymbol{\Phi}^{-}_{0} = \mathbf{I} \tag{15A}$$

$$\boldsymbol{\Lambda}^{-}_{\ell,\,k} = \mathbf{F}_{k-1} \boldsymbol{\Lambda}_{\ell,\,k-1} \quad , \quad k > 0 \tag{16A}$$

$$\boldsymbol{\Lambda}^{-}_{\ell,\,k} = \mathbf{F}_{k-1} \boldsymbol{\Lambda}_{\ell,\,k-1} \quad , \quad k > 0 \tag{17A}$$

Appendix B

This appendix derives an alternative expression for the true estimate error variance $\sigma^2_{y,k}$. In Eq. (39), $\sigma^2_{y,k}$ was shown to be equal to

$$\sigma^2_{y,k} = \boldsymbol{\alpha}_y^T \, \boldsymbol{\Phi}_k \, \mathbf{P}_0^{-} \, \boldsymbol{\Phi}_k^T \, \boldsymbol{\alpha}_y + \sum_{\substack{j=1 \\ k \neq 0}}^{n_w} \boldsymbol{\alpha}_y^T \, \boldsymbol{\Gamma}_{j,k} \, \mathbf{W}_{j,k-1} \boldsymbol{\Gamma}_{j,k}^T \, \boldsymbol{\alpha}_y + \sum_{\ell=1}^{n_v} \boldsymbol{\alpha}_y^T \, \boldsymbol{\Lambda}_{\ell,k} \, \mathbf{V}_{\ell,k} \, \boldsymbol{\Lambda}_{\ell,k}^T \, \boldsymbol{\alpha}_y \quad , \quad k \geq 0 \tag{1B}$$

where $\boldsymbol{\alpha}_y$ is an $n_x \times 1$ vector, $\boldsymbol{\Phi}_k$ is an $n_x \times n_x$ matrix, $\mathbf{P}_0^{-}$ is an $n_x \times n_x$ matrix, $\boldsymbol{\Gamma}_{j,k}$ is an $n_x \times k$ matrix, $\mathbf{W}_{j,k-1}$ is a $k \times k$ matrix, $\boldsymbol{\Lambda}_{\ell,k}$ is an $n_x \times (k + 1)$ matrix and $\mathbf{V}_{\ell,k}$ is a $(k + 1) \times (k + 1)$ matrix.

The first sum on the right hand side of Eq. (1B) is a sum of quadratic forms, each of which can be written as

$$\boldsymbol{\alpha}_y^T \, \boldsymbol{\Gamma}_{j,k} \, \mathbf{W}_{j,k-1} \boldsymbol{\Gamma}_{j,k}^T \, \boldsymbol{\alpha}_y = \sum_{mn} [\, (\, \boldsymbol{\Gamma}_{j,k}^T \, \boldsymbol{\alpha}_y \, \boldsymbol{\alpha}_y^T \, \boldsymbol{\Gamma}_{j,k} \,) \circ \mathbf{W}_{j,k-1} \,]_{mn} \tag{2B}$$

where m and n are matrix row and column indices, respectively, and $\circ$ indicates the entrywise product of two matrices, defined as $[\, \mathbf{A} \circ \mathbf{B} \,]_{mn} = a_{mn} \, b_{mn}$.

Defining the $k \times k$ matrix $\boldsymbol{\Pi}_{j,k} = \boldsymbol{\Gamma}_{j,k}^T \, \boldsymbol{\alpha}_y \, \boldsymbol{\alpha}_y^T \, \boldsymbol{\Gamma}_{j,k}$ simplifies Eq. (2B) to the form

$$\boldsymbol{\alpha}_y^T \, \boldsymbol{\Gamma}_{j,k} \, \mathbf{W}_{j,k-1} \boldsymbol{\Gamma}_{j,k}^T \, \boldsymbol{\alpha}_y = \sum_{mn} [\, \boldsymbol{\Pi}_{j,k} \circ \mathbf{W}_{j,k-1} \,]_{mn} \tag{3B}$$

In order to observe the nature of $\sum_{mn} [\, \boldsymbol{\Pi}_{j,k} \circ \mathbf{W}_{j,k-1} \,]_{mn}$, the subscript j will temporarily be dropped. From Eq. (38), the matrix $\mathbf{W}_{k-1}$ was shown to have the symmetric Toeplitz structure

$$\mathbf{W}_{k-1} = \begin{bmatrix} \overset{w}{r}_0 & \overset{w}{r}_1 & \overset{w}{r}_2 & \cdots & \overset{w}{r}_{k-1} \\ \overset{w}{r}_1 & \overset{w}{r}_0 & \overset{w}{r}_1 & \ddots & \vdots \\ \overset{w}{r}_2 & \overset{w}{r}_1 & \overset{w}{r}_0 & \ddots & \overset{w}{r}_2 \\ \vdots & \ddots & \ddots & \ddots & \overset{w}{r}_1 \\ \overset{w}{r}_{k-1} & \cdots & \overset{w}{r}_2 & \overset{w}{r}_1 & \overset{w}{r}_0 \end{bmatrix} \tag{4B}$$

Because the elements of $\mathbf{W}_{k-1}$ are identical along any given diagonal, the sum of the elements of the entrywise product $\mathbf{\Pi}_k \circ \mathbf{W}_{k-1}$ can be written in the form

$$\sum_{mn} [\, \mathbf{\Pi}_k \circ \mathbf{W}_{k-1} \,]_{mn} = (\, p_{11} + p_{22} + \cdots + p_{kk} \,) \overset{w}{r}_0 + 2(\, p_{12} + p_{23} + \cdots + p_{(k-1)k} \,) \overset{w}{r}_1 + 2(\, p_{13} + p_{24} + \cdots + p_{(k-2)k} \,) \overset{w}{r}_2 + \cdots + 2 p_{1k} \overset{w}{r}_{k-1} \tag{5B}$$

where p_{ij} is the (i , j) element of $\mathbf{\Pi}_k$.

Reinstating the subscript j, Eq. (5B) implies that Eq. (3B) can be expressed as

$$\boldsymbol{\alpha}_y^T \mathbf{\Gamma}_{j,k} \, \mathbf{W}_{j,k-1} \mathbf{\Gamma}_{j,k}^T \, \boldsymbol{\alpha}_y = \sum_{s=0}^{k-1} \overset{w}{\gamma}_{j,s} \overset{w}{r}_{j,s} \tag{6B}$$

where $\overset{w}{\gamma}_{j,0}$ is the sum of the elements along the main diagonal of $\mathbf{\Pi}_{j,k}$, $\overset{w}{\gamma}_{j,1}$ is twice the sum of the elements along the first super diagonal of $\mathbf{\Pi}_{j,k}$, $\overset{w}{\gamma}_{j,2}$ is twice the sum of the elements along the second super diagonal of $\mathbf{\Pi}_{j,k}$, etc.

The same procedure can be applied to the second summation on the right hand side of Eq. (1B), resulting in the final expression

$$\sigma_{y,k}^2 = \boldsymbol{\alpha}_y^T \mathbf{\Phi}_k \, \mathbf{P}_0^- \, \mathbf{\Phi}_k^T \, \boldsymbol{\alpha}_y + \sum_{j=1}^{n_w} \sum_{\substack{s=0 \\ k \neq 0}}^{k-1} \overset{w}{\gamma}_{j,s} \overset{w}{r}_{j,s} + \sum_{\ell=1}^{n_v} \sum_{u=0}^{k} \overset{v}{\gamma}_{\ell,u} \overset{v}{r}_{\ell,u} \quad , \quad k \geq 0 \tag{7B}$$

which is equivalent to the expression given in Eq. (40).

Appendix C

This appendix derives the discrete-time autocorrelation function of the integrated random process

$$w_k = \int_{t_k}^{t_k+\Delta t} [\xi(\tau) + q_\theta(\tau)]d\tau \tag{1C}$$

where $\xi(t)$ is a first order Gauss-Markov process, $q_\theta(t)$ is a zero-mean, Gaussian white noise process and Δt is the discrete-time sampling interval. The autocorrelation function of $q_\theta(t)$ is given by

$$E[q_\theta(t_1)q_\theta(t_2)] = Q_\theta \delta(t_1 - t_2) \tag{2C}$$

where Q_θ is the power spectral density of the white noise process and $\delta(t)$ is the Dirac delta function. For the first order Gauss-Markov process, the autocorrelation function is given as [28]

$$E[\xi(t_1)\xi(t_2)] = \sigma_\xi^2 \exp\left(-\frac{|t_1 - t_2|}{\tau_\xi}\right) \tag{3C}$$

where σ_ξ^2 and τ_ξ are the variance and time constant of the process, respectively.

Now consider the values of *w* at time index *k* and time index ℓ.

$$w_k = \int_{t_k}^{t_k+\Delta t} [\xi(u) + q_\theta(u)]du \tag{4C}$$

$$w_\ell = \int_{t_\ell}^{t_\ell+\Delta t} [\xi(u) + q_\theta(u)]du \tag{5C}$$

The discrete-time autocorrelation function of *w* is defined as $E[w_k w_\ell]$. From Eqs. (4C) and (5C), this expectation can be written as

$$E[w_k w_\ell] = \int_{t_\ell}^{t_\ell+\Delta t} \int_{t_k}^{t_k+\Delta t} E\{[\xi(u) + q_\theta(u)][\xi(v) + q_\theta(v)]\}du\, dv. \tag{6C}$$

Assuming that $\xi(t)$ and $q_\theta(t)$ are mutually uncorrelated, Eq. (6C) can be expanded into the form

$$E[w_k w_\ell] = \int_{t_\ell}^{t_\ell+\Delta t} \int_{t_k}^{t_k+\Delta t} E[\xi(u)\,\xi(v)]du\, dv + \int_{t_\ell}^{t_\ell+\Delta t} \int_{t_k}^{t_k+\Delta t} E[q_\theta(u)\, q_\theta(v)]du\, dv. \tag{7C}$$

For simplicity, Eq. (7C) will be written in the form $E[\,w_k\,w_\ell\,] = I_1 + I_2$.

In order to compute I_1, the integral must be evaluated separately for the cases $\ell = k$ and $\ell > k$ because of the absolute value in Eq. (3C). For $\ell = k$, substituting the right hand side of Eq. (3C) into Eq. (7C) results in

$$I_1 = \int_{t_\ell}^{t_\ell+\Delta t}\int_{t_\ell}^{t_\ell+\Delta t} \sigma_\xi^2 \exp\left(-\frac{|\,u-v\,|}{\tau_\xi}\right) du\; dv\,. \tag{8C}$$

The absolute value can be eliminated by writing I_1 as the sum of two integrals

$$I_1 = \int_{t_\ell}^{t_\ell+\Delta t}\int_{t_\ell}^{v} \sigma_\xi^2 \exp\left(-\frac{v-u}{\tau_\xi}\right) du\; dv + \int_{t_\ell}^{t_\ell+\Delta t}\int_{v}^{t_\ell+\Delta t} \sigma_\xi^2 \exp\left(-\frac{u-v}{\tau_\xi}\right) du\; dv\,. \tag{9C}$$

It is straightforward to verify that the integrals evaluate to the expression

$$I_1 = 2\,(\sigma_\xi\,\tau_\xi)^2\left[\,\frac{\Delta t}{\tau_\xi} - 1 + \exp\left(-\frac{\Delta t}{\tau_\xi}\right)\right] \quad , \quad \ell = k\,. \tag{10C}$$

Considering the case now where $\ell > k$, I_1 becomes

$$I_1 = \int_{t_\ell}^{t_\ell+\Delta t}\int_{t_k}^{t_k+\Delta t} \sigma_\xi^2 \exp\left(-\frac{v-u}{\tau_\xi}\right) du\; dv\,. \tag{11C}$$

It is straightforward to show that the double integral in Eq. (11C) evaluates to

$$I_1 = (\sigma_\xi\,\tau_\xi)^2 \exp\left(-\frac{t_\ell - t_k}{\tau_\xi}\right)\left[\,1-\exp\left(-\frac{\Delta t}{\tau_\xi}\right)\right]\left[\,\exp\left(\frac{\Delta t}{\tau_\xi}\right)-1\,\right] \quad , \quad \ell > k\,. \tag{12C}$$

Because the autocorrelation function is symmetric about the origin, the case where $\ell < k$ is easily handled by changing the argument $t_\ell - t_k$ to $t_k - t_\ell$ in Eq. (12C). In addition, for periodic sampling, $t_\ell - t_k$ can be written as a multiple of the sampling interval, Δt. That is, $t_\ell - t_k = s\Delta t$. Therefore, in general, I_1 can be written as

$$I_1 = \begin{cases} 2\,(\sigma_\xi\,\tau_\xi)^2\left[\,\dfrac{\Delta t}{\tau_\xi} - 1 + \exp\left(-\dfrac{\Delta t}{\tau_\xi}\right)\right] & , \quad s = 0 \\ (\sigma_\xi\,\tau_\xi)^2 \exp\left(-\dfrac{|\,s\Delta t\,|}{\tau_\xi}\right)\left[\,1-\exp\left(-\dfrac{\Delta t}{\tau_\xi}\right)\right]\left[\,\exp\left(\dfrac{\Delta t}{\tau_\xi}\right)-1\,\right] & , \quad s \neq 0 \end{cases}. \tag{13C}$$

Substituting Eq. (2C) into the second integral on the right hand side of Eq. (7C) and using the fact that Q_θ is a constant yields

$$I_2 = Q_\theta \int_{t_\ell}^{t_\ell+\Delta t} \int_{t_k}^{t_k+\Delta t} \delta(u-v)\, du\, dv\,. \tag{14C}$$

Because the Dirac delta function is non-zero only when $u = v$, the double integral in Eq. (14C) is non-zero only when $\ell = k$ (i.e., $s = 0$). Therefore, I_2 evaluates to

$$I_2 = \begin{cases} Q_\theta \Delta t & , \quad s = 0 \\ 0 & , \quad s \neq 0 \end{cases}. \tag{15C}$$

Combining Eqs. (13C) and (15C) results in the complete autocorrelation function

$$r_s = \begin{cases} 2(\sigma_\xi\, \tau_\xi)^2 \left[\dfrac{\Delta t}{\tau_\xi} - 1 + \exp\left(-\dfrac{\Delta t}{\tau_\xi} \right) \right] + Q_\theta \Delta t & , \quad s = 0 \\ (\sigma_\xi\, \tau_\xi)^2 \exp\left(-\dfrac{|\, s\Delta t\,|}{\tau_\xi} \right) \left[1 - \exp\left(-\dfrac{\Delta t}{\tau_\xi} \right) \right] \left[\exp\left(\dfrac{\Delta t}{\tau_\xi} \right) - 1 \right] & , \quad s \neq 0 \end{cases} \tag{16C}$$

Acknowledgements

We would like to thank our research sponsors at the Naval Air Systems Command for sponsoring this research.

References

[1] Anderson, B. D. O., and Moore, J. B., *Optimal Filtering*, Dover Publications, New York, 1979, Chap. 11.

[2] Bryson, A. E., and Henrikson, L. J., "Estimation Using Sampled Data Containing Sequentially Correlated Noise," *Journal of Spacecraft and Rockets*, Vol. 5, No. 6, 1968, pp. 662-665.

[3] Schmidt, S., "Applications of State-Space Methods to Navigation Problems," *Advances in Control Systems*, edited by C. T. Leondes, Vol. 3, Academic Press, New York, 1966, pp. 293-340.

[4] DeCleene, B., "Defining Pseudorange Integrity – Overbounding," *Proceedings of the 13th International Technical Meeting of the Satellite Division of the Institute of Navigation*, Inst. of Navigation, 2000, pp. 1916-1924.

[5] Rife, J., Pullen, S., Pervan, B., and Enge, P., "Paired Overbounding and Application to GPS Augmentation," *Proceedings of the IEEE Position, Location and Navigation Symposium*, IEEE, 2004, pp. 439-446.

[6] Rife, J., and Gebre-Egziabher, D., "Symmetric Overbounding of Correlated Errors," *NAVIGATION*, Vol. 54, No. 2, 2007, pp. 109-124.

[7] Pullford, G. W., "A Proof of the Spherically Symmetric Overbounding Theorem for Linear Systems," *NAVIGATION*, Vol. 55, No. 4, 2008, pp. 283-292.

[8] Khanafseh, S., Langel, S., and Pervan, B., "Overbounding Position Errors in the Presence of Carrier Phase Multipath Error Model Uncertainty," *Proceedings of the IEEE/ION Position, Location and Navigation Symposium*, IEEE, 2010, pp. 575-584.

[9] Langel, S., Khanafseh, S., and Pervan, B., "Bounding Integrity Risk in the Presence of Parametric Time Correlation Uncertainty," *Proceedings of the 2012 International Technical Meeting of the Institute of Navigation*, Inst. of Navigation, 2012, pp. 1666-1680.

[10] Xie, L., "On Robust H2 Estimation," *ACTA Automatica Sinica*, Vol. 31, No. 1, 2005, pp. 1-12.

[11] Xie, L., de Souza, C. E., and Fu, M., "H_∞ Estimation for Discrete-Time Linear Uncertain Systems," *International Journal of Robust and Nonlinear Control*, Vol. 1, No. 2, 1991, pp. 111-123.

[12] Xie, L., Soh, Y. C., and de Souza, C. E., "Robust Kalman Filtering for Uncertain Discrete-Time Systems," *IEEE Transactions On Automatic Control*, Vol. 39, No. 6, 1994, pp. 1310-1314.

[13] Petersen, I. R., and McFarlane, D. C., "Optimal Guaranteed Cost Filtering for Uncertain Discrete-Time Linear Systems," *International Journal of Robust and Nonlinear Control*, Vol. 6, No. 4, 1996, pp. 267-280.

[14] Zhu, X., Soh, Y. C., and Xie, L., "Design and Analysis of Discrete-Time Robust Kalman Filters," *Automatica*, Vol. 38, No. 6, 2002, pp. 1069-1077.

[15] Geromel, J. C., and de Oliveira, M. C., "H_2 and H_∞ Robust Filtering for Convex Bounded Uncertain Systems," *Proceedings of the 37th IEEE Conference on Decision and Control*, IEEE, 1998, pp. 146-151.

[16] Tuan H. D., Apkarian, P., and Nguyen, T. Q., "Robust and Reduced-Order Filtering: New LMI-Based Characterizations and Methods," *IEEE Transactions on Signal Processing*, Vol. 49, No. 12, 2001, pp. 2975-2984.

[17] Geromel, J., Bernussou, J., Garcia, G., and de Oliveira, M. C., "H_2 and H_∞ Robust Filtering for Discrete-Time Linear Systems," *SIAM Journal on Control and Optimization*, Vol. 38, No. 5, 2000, pp. 1353-1368.

[18] Shaked, U., Xie, L., and Soh, Y. C., "New Approaches to Robust Minimum Variance Filter Design," *IEEE Transactions on Signal Processing*, Vol. 49, No. 11, 2001, pp. 2620-2629.

[19] Xie, L., Lu, L., Zhang, D., and Zhang, H., "Improved Robust H_2 and H_∞ Filtering for Uncertain Discrete-Time Systems," *Automatica*, Vol. 40, No. 5, 2004, pp. 873-880.

[20] Geromel, J., de Oliveira, M. C., and Bernussou, J., "Robust Filtering of Discrete-Time Linear Systems with Parameter Dependent Lyapunov Functions," *SIAM Journal on Control and Optimization*, Vol. 41, No. 3, 2002, pp. 700-711.

[21] Boyd, S., El Ghaoui, L., Feron, E., and Balakrishnan, V., "Linear Matrix Inequalities in System and Control Theory," *SIAM Studies in Applied Mathematics*, Vol. 15, SIAM, Philadelphia, 1994.

[22] Lewis, F. L., Xie, L., and Popa, D., *Optimal and Robust Estimation*, 2nd Ed., CRC Press, Boca Raton, 2008.

[23] Chan, F. C., Joerger, M., and Pervan, B., "High Integrity Stochastic Modeling of GPS Receiver Clock for Improved Positioning and Fault Detection Performance," *Proceedings of the IEEE/ION Position, Location and Navigation Symposium*, IEEE, 2010, pp. 1245-1257.

[24] Brown, R. G., and Hwang, P. Y. C., *Introduction to Random Signals and Applied Kalman Filtering*, 3rd Ed., John Wiley & Sons, New York, 1997, Chap. 5.

[25] Chen, C. T., *Linear System Theory and Design*, 3rd Ed., Oxford University Press, New York, 1999, Chap. 2.

[26] Stengel, R. F., *Optimal Control and Estimation*, Dover Publications, New York, 1994, Chap. 2.

[27] Van Loan , C. F., "Computing Integrals Involving the Matrix Exponential," *IEEE Transactions on Automatic Control*, Vol. ac-23, No. 3, 1978, pp. 395-404.

[28] Technical Staff, The Analytic Sciences Corporation, *Applied Optimal Estimation*, edited by A. Gelb, The M.I.T. Press, Cambridge, USA, 1974, Chap. 1.